

This work was written as part of one of the author's official duties as an Employee of the United States Government and is therefore a work of the United States Government. In accordance with 17 U.S.C. 105, no copyright protection is available for such works under U.S. Law.

Public Domain Mark 1.0

<https://creativecommons.org/publicdomain/mark/1.0/>

Access to this work was provided by the University of Maryland, Baltimore County (UMBC) ScholarWorks@UMBC digital repository on the Maryland Shared Open Access (MD-SOAR) platform.

**Please provide feedback**

Please support the ScholarWorks@UMBC repository by emailing [scholarworks-group@umbc.edu](mailto:scholarworks-group@umbc.edu) and telling us what having access to this work means to you and why it's important to you. Thank you.



## Plasma ion composition measurements for Europa

E.C. Sittler Jr.<sup>a,\*</sup>, J.F. Cooper<sup>a</sup>, R.E. Hartle<sup>a</sup>, W.R. Paterson<sup>a</sup>, E.R. Christian<sup>a</sup>, A.S. Lipatov<sup>b</sup>,  
P.R. Mahaffy<sup>a</sup>, N.P. Paschalidis<sup>a</sup>, M.A. Coplan<sup>c</sup>, T.A. Cassidy<sup>d</sup>, J.D. Richardson<sup>e</sup>,  
B. Fegley Jr.<sup>f</sup>, N. Andre<sup>g</sup>

<sup>a</sup> NASA Goddard Space Flight Center, Greenbelt, MD 20771, USA

<sup>b</sup> GPHI/University of Maryland Baltimore County, Baltimore, MD USA

<sup>c</sup> University of Maryland, College Park, MD, USA

<sup>d</sup> Laboratory for Atmospheric and Space Physics (LASP), University of Colorado, Boulder, CO, USA

<sup>e</sup> Massachusetts Institute of Technology, Cambridge, MA, USA

<sup>f</sup> Washington University, St. Louis, MO, USA

<sup>g</sup> CESR/IRAP, Toulouse, France

### ARTICLE INFO

#### Article history:

Received 13 October 2012

Received in revised form

29 January 2013

Accepted 30 January 2013

Available online 13 March 2013

#### Keywords:

Europa Magnetospheric interaction

Ionospheric currents

Surface composition

Oceanic fields

### ABSTRACT

Jupiter magnetospheric interactions and surface composition, both important to subsurface ocean detection for the Galilean icy moons Europa, Ganymede, and Callisto, can be measured using plasma ion mass spectrometry on either an orbiting spacecraft or one designed for multiple flybys of these moons. Detection of emergent oceanic materials at the Europa surface is more likely than at Ganymede and Callisto. A key challenge is to resolve potential intrinsic European materials from the space weathering patina of iogenic species implanted onto the sensible surface by magnetospheric interactions. Species-resolved measurements of pickup ion currents are also critical to extraction of oceanic induced magnetic fields from magnetospheric interaction background dominated by these currents. In general the chemical astrobiological potential of Europa should be determined through the combination of surface, ionospheric, and pickup ion composition measurements. The requisite Ion Mass Spectrometer (IMS) for these measurements would need to work in the high radiation environment of Jupiter's magnetosphere between the orbits of Europa and Ganymede, and beyond. A 3D hybrid model of the moon-magnetosphere interaction is also needed to construct a global model of the electric and magnetic fields, and the plasma environment, around Europa. Europa's ionosphere is probably usually dominated by hot pickup ions with 100–1000 eV temperatures, excursions to a “classical” cold ionosphere likely being infrequent. A field aligned ionospheric wind driven by the electron polarization electric field should arise and be measurable.

Published by Elsevier Ltd.

## 1. Introduction

### 1.1. Europa exogenic and endogenic compositional signatures, magnetospheric interaction correction currents and ocean characterization

The ocean moon Europa remains the highest priority destination for future spacecraft missions to the Jupiter system as recommended by the last two planetary science decadal surveys of the U.S. Academies of Science National Research Council (Belton et al., 2002; Squyres et al., 2011). While the varying and complex visible surface geology of Europa offer a rich target of investigation for fully instrumented missions (e.g., Greeley et al., 2009) including a full range of remote sensing and in-situ measurements, the true physical

and chemical characteristics of the unseen but strongly suspected (Pappalardo et al., 1999; Greeley et al., 2004, 2009; Alexander et al., 2009) subsurface ocean remain unknown. The geologic evidence is consistent with (but not yet definitive proof of) the existence of an ocean driving formation of visible surface features over the past tens of millions of years or earlier, but only the detection of induced magnetic fields (Khurana et al., 1998; Kivelson et al., 1999, 2000) from magnetospheric interaction with the presumably salty ocean indicates presence of a modern ocean. However, models of the magnetospheric interaction (Saur et al., 1998; Lipatov et al., 2010) indicate that plasma currents above the surface constitute major backgrounds for detection of the intrinsic oceanic signals, so this background, as determined by in-situ plasma current measurements and associated models, must first be subtracted to set limits on the oceanic source of induced magnetic field.

The prime objective for this paper is clarification about these details of the local magnetospheric and ionospheric backgrounds impacting understanding of the past measurements by Galileo and

\* Corresponding author. Tel.: +1 301 286 9215; fax: +1 301 286 1648.  
E-mail address: Edward.C.Sittler@nasa.gov (E.C. Sittler Jr.).

as input to scientific instrument requirements for future missions to Europa. Although geologic evidence strongly suggests oceanic activity in the recent geologic past, the Galileo magnetometer measurements of apparently induced magnetic fields provide critical support to the model of a presently existing modern ocean. Any future mission to characterize the ocean through magnetic field measurements must also provide supporting measurements of the plasma ion and electron currents comprising the background environment above the moon surface. It is also essential to measure the composition of the ionic and neutral species ejected from the surface by sputtering to search for oceanic materials potentially emergent to the surface. The challenge on the composition measurements is to find these endogenic materials amidst the background of magnetospheric species constantly raining down on the surface. It is also essential to characterize the compositional abundances of the magnetospheric ions so these can be subtracted out from the surface composition to reveal the presence of oceanic materials.

The detected presence of sulfate hydrates (McCord et al., 1998, 1999; Carlson et al., 1999, 2002) on the surface of Europa could indicate chemical communication between an underlying salty ocean and the sensible surface, but here also is the need to subtract off the background from magnetospheric interaction. Io dumps about one metric ton per second of volcanic ejecta into the Jupiter magnetosphere and a tiny  $\sim 10^{-5}$  fraction of this iogenic material impacts Europa with potentially very significant contributions to the chemistry of the moon's surface. In order to measure intrinsic composition of Europa and the other moons, one must first understand the transport of iogenic plasma from Io's torus to these moons and then secondly determine what fraction of this iogenic plasma reaches the surface by both measuring the interaction and using a 3D hybrid simulation of the interaction, e.g., by Lipatov et al. (2010). The bulk flow of plasma is dominated by highly abundant atomic and molecular ions of iogenic sulphur and oxygen; protons are a minor contributor. Oxygen is by mass the dominant elemental constituent of the Europa surface and therefore provides the best reference for abundance measurements of all other major, minor, and trace species.

A key measurement challenge is to resolve the minor and trace abundances of other species against this highly dominant sulphur and oxygen background. The most informative species for chemical evolution and astrobiology may only be detected at parts per million or less. In order to separate the iogenic and intrinsic species the ratios of major ions such as  $O^+/S^{++}$  and  $O_2^+/S^+$  should be determined. Even more importantly, the plasma measurements must determine the background current contributions from

species-resolved hot ionospheric and pickup ions (PUI), i.e.,  $O_2^+$ , to enable extraction of oceanic induced magnetic fields from varying interactions of the magnetosphere's magnetic field with the apparently conducting salty ocean of Europa.

## 1.2. In situ plasma suite for future missions to Europa, Ganymede and Callisto

In this paper we quantitatively consider details of the magnetospheric, ionospheric, neutral atmospheric, and surface interactions that would be applicable to a suggested suite of plasma sensors on future missions to Europa, Ganymede, Callisto, and their orbital environments in the Jupiter magnetosphere. Although we understand that a significantly descope payload may not allow all of these sensors, the suggested baseline suite for our present discussion consists of the following four sensors (see Table 1): (1) 3D Ion Mass Spectrometer (IMS) with minor ion detection capability for the magnetospheric core plasma dominating the density and momentum of the flow (see Belcher, 1983 and Paterson et al., 1999 for their properties) with energy range  $1 \text{ V} \leq E/Q \leq 30 \text{ kV}$ , (2) energetic Ion and Electron Sensor (IES) to measure the dominant suprathermal ion component of magnetospheric plasma pressure at all the icy moons except for Io (see Mauk et al., 1996, 2004; Cooper et al., 2001; Paranicos et al., 2009 for their properties), (3) 3D Plasma Electron Spectrometer (ELS) for electrons with energy range  $1 \text{ eV} \leq E \leq 30 \text{ keV}$  to model the ionization rate of Europa's exosphere (i.e., source rate for pickup ions and their currents) and ambipolar electric fields along field lines, and (4) Magnetometer to measure Jupiter's intrinsic magnetic field, the global currents of its magnetosphere and the magnetic field properties around Europa. The suggested suite could be further enhanced with a 3D Neutral Mass Spectrometer (3D-NMS) for detection of sputtered neutrals with  $<0.1 \text{ eV}$  energies (Cassidy et al., 2007, 2009; Johnson et al., 2009; Plainaki et al., 2012) expected at Europa. It would then be useful for energetic neutral atom (ENA) and molecule measurements of species directly sputtered from the moon surface and exosphere. Although compositions of the relatively colder neutral atmospheres and ionospheres of Saturnian moons have been successfully measured with flyby measurements by the Cassini Ion Neutral Mass Spectrometer (Waite et al., 2006; 2009), this instrument with its narrow field of view (FOV) (Waite et al. 2004) would be less useful for measurements of exospheric ions and neutrals at orbital speeds  $\sim 1\text{--}2 \text{ km/s}$ . The relatively hotter exospheric environment at Europa and other Galilean moons requires a much wider FOV and full spectral coverage at eV–keV energies.

**Table 1**  
In situ plasma suite parameters.

Sensor	IMS	ELS	IES Ions	IES electrons
Energy range	$1 \text{ V} \leq E/Q \leq 30 \text{ kV}$	$1 \leq E \leq 30 \text{ keV}$	$20 \text{ keV} \leq E \leq 10 \text{ MeV}$	$20 \text{ keV} \leq E \leq 2 \text{ MeV}$
Energy resolution	$\Delta E/E \sim 10\%$	$\Delta E/E \sim 10\%$	$\Delta E/E \sim 30\%$	$\Delta E/E \sim 30\%$
FOV coverage	$360^\circ \times 90^\circ$ Centered on co-rotation direction and nadir direction	$360^\circ \times 90^\circ$	$180^\circ$ in plane Centered on co-rotating flow and PAD <sup>1</sup>	$180^\circ$ in plane Measure PAD <sup>1</sup>
Angular resolution	$\Delta\alpha \times \Delta\beta \sim 22.5^\circ \times 5^\circ$	$\Delta\alpha \times \Delta\beta \sim 22.5^\circ \times 5^\circ$	$\Delta\alpha \times \Delta\beta \sim 20^\circ \times 20^\circ$	$\Delta\alpha \times \Delta\beta \sim 10^\circ \times 20^\circ$
Mass range	$1 \leq M/Q \leq 100$	Measure negative ions desired (discovery mode) $M/\Delta M \sim 5$		
Mass resolution	$10 \leq M/\Delta M \leq 60$	$10^{-4} \text{ cm}^2\text{-ster-eV/eV}$	$10^{-2} \text{ to } 10^8 \text{ ions}/(\text{cm}^2\text{-s-sr-MeV})$	$10^2 \text{ to } 10^9 \text{ electrons}/(\text{cm}^2\text{-s-sr-MeV})$
GF for IMS/ELS intensities (IES)	$10^{-4} \text{ cm}^2\text{-ster-eV/eV}$			
Ions desired to resolve	$H_2^+/^4He^{++}, O^+/S^{++}, O_2^+/S^+$		Resolve H, He, O and S	
Time resolution	Major ions: 1–10 s minor ions: 1–60 min	1–10 s	1–10 s	1–10 s

<sup>1</sup> PAD = Pitch Angle Distribution.

### 1.3. Global 3D model of electric and magnetic fields and PUI trajectories and origins

The IMS can supplement other measurements of surface composition, e.g., remote IR–UV spectroscopic mapping, but uniquely provides much higher mass resolution for elemental and molecular identification than is possible from remote measurements. Secondary ion mass spectrometry (SIMS) is one of the ground-based laboratory techniques cited in the Mars sample return studies of Squyres et al. (2011) but the IMS measurement of naturally sputtered material from the Galilean moons and other planetary bodies is essentially the same approach and does not require sample return. For example the composition of sulphate salts on the surface of Europa have variously been inferred from near-infrared spectrometry (Carlson et al., 1998, 2002; McCord et al., 1998, 1999; Dalton et al., 2010) to be associated with  $\text{H}_2\text{SO}_4$ ,  $\text{MgSO}_4$ , or  $\text{Na}_2\text{SO}_4$ , or some combination thereof, but the precise abundances of these molecules and constituent elements have not been determined. IMS orbital or flyby measurement of the ions is enabled by neutral atomic and molecular species ejection by sputtering off the moon surfaces, ionization in the local plasma environment, and immediate acceleration as pickup ions (PUI) in the corotating planetary magnetic field. The local plasma flow velocity  $\mathbf{V}$  is first measured to model the interaction between Europa and Jupiter's fast rotating magnetosphere. From knowledge of  $\mathbf{V}$  the convective electric field can be estimated via the relationship  $\mathbf{E} = -\mathbf{V} \times \mathbf{B}$ . The convective electric field accelerates the pickup ions up to the spacecraft location, which enables the in-situ measurement by IMS. The IES provides key measurements for modelling of the moon-magnetosphere interaction, since energetic ( $>10$  keV) ions dominate the magnetosphere's plasma pressure at Europa with ion gyro-radii  $\sim 500$  km, these same ions dominate the sputtering rates for Europa's exosphere, and energetic (keV–MeV) electrons dominate the radiolytic processes on Europa's surface. The plasma electrons drive the ionization of Europa's exosphere (see Sittler and Strobel, 1987 and Saur et al., 1998) and can produce field-aligned ionospheric outflows arising from a polarization electric field (see Sittler et al., 2010 and Coates et al., 2012 for observed ionospheric outflows from Titan).

Three-dimensional computational models extend the in-situ measurements along the spacecraft orbit to simulation of the global field and plasma environment around the moon. Hybrid kinetic 3D models (Lipatov et al., 2010) of the moon-magnetosphere interaction can be utilized with plasma and magnetometer measurements to construct global models of the electric and magnetic fields around Europa. A single-fluid 3D MHD model of the plasma interaction, including induced fields from the sub-surface ocean, has been developed by Schilling et al. (2007, 2008) but does not account for the kinetic motions of ions with relatively large magnetic gyroradii. These motions produce asymmetries in the PUI density and velocity distributions around the moon. We use the 3D hybrid kinetic model approach (Lipatov et al., 2010, 2013) that more accurately simulates the ion kinetics while still treating electrons in the fluid approximation with the forced assumption of charge neutrality. Boundary conditions for these global models are first set from upstream field and plasma measurements and then the computed 3-D distributions are used with single-ion trajectory algorithms to trace PUI events back from the spacecraft to formation sites at Europa's surface or in the moon's exosphere.

Since the envisioned IMS has a minor-trace ion detection capability in a high radiation environment, elemental and isotopic analysis of potentially extruded oceanic materials at the moon surfaces becomes possible; this would further support the ocean objectives (Hand et al., 2009). We judge that an ideal height for such measurements from a polar orbiting spacecraft about Europa

is  $z \sim 100$ – $200$  km (see Clark et al., 2009). The ejecta produced by sputtering of the surfaces of Europa have been shown to be representative of the surface composition (Johnson et al., 2009). Trace back of the PUI events to sputtering source regions allows surface compositional mapping at surface horizontal resolution comparable to the spacecraft altitude, this resolution is limited by angular resolution of typical IMS measurements and by knowledge of the fields along the aperture-averaged trace back trajectories. Europa's patchy  $\text{O}_2$  exosphere dominates over other neutral components and will determine the interaction with Jupiter's magnetosphere (see McGrath et al., 2009), most importantly including pickup ion current contributions to the magnetic field environment.

### 1.4. Ionospheric layer and PUI detection

Among the greatest uncertainties in current models for the moon-magnetosphere interaction at Europa are the parameters of the ionospheric layer between the impinging magnetospheric environment and the solid surface. The ionospheric species arise from UV or plasma ionization of neutral atmospheric molecules sputtered off the surface by magnetospheric ion irradiation. One such critical parameter is the height above the surface and thickness of the “ionopause”, the transitional region between ions of magnetospheric and ionospheric origin. The critical parameters for measuring Europa's surface composition from IMS measurements of PUIs are the height of the “ionopause” boundary  $Z_{\text{ion}}$  and its thickness  $\Delta Z_{\text{ion}}$  if this boundary does exist. Below a classical ionopause the external plasma flow is stopped, the convective electric field of the external flow is near zero, the gyro-radius,  $r_g$ , of the local PUIs is essentially zero, and the ionosphere below this boundary is very cold with temperature  $T_{\text{ion}} < 1$  eV. Even if such a boundary forms above spacecraft altitude  $\sim 100$ – $200$  km, the “ionopause” thickness is expected to be  $\Delta Z_{\text{ion}} \sim r_g$  of external flow with  $r_g \sim 30$  km for cold plasma and  $\sim 500$  km for hot plasma. If thickness  $\Delta Z_{\text{ion}} > Z_{\text{ion}}$ , then the classical ionopause does not occur and convective electric fields of external flow can penetrate down to the moon's surface. Present 3D MHD models by Schilling et al. (2007, 2008) with spatial resolutions  $\sim 80$  km, and 3D hybrid models by Lipatov et al. (2010) with spatial resolution  $\sim 150$  km, cannot reliably resolve the ionopause boundary height and thickness. Since Schilling et al. (2007, 2008) use MHD calculations that intrinsically assume zero gyroradius for ions, their model cannot resolve  $\Delta Z_{\text{ion}}$  even with high spatial resolution. Only the hybrid kinetic models have the potential for doing this.

The models show that the external magnetic field penetrates down to the surface and passes through the moon (Schilling et al., 2007, 2008; Lipatov et al., 2010), so magnetospheric electrons can move along magnetic field lines and have direct access to the ion exosphere. Therefore, ionospheric electrons will be relatively hot  $T_e \sim 5$ – $10$  eV (see Saur et al., 1998). As noted above and later quantified these hot ionosphere electrons, can pull ions out of the ionosphere along the magnetic field via a field-aligned polarization electric field (see Sittler et al., 2010 for Titan) and form a polar wind. These ions could be observed by the IMS, even for flyby missions through the Alfvén wings, as an outward flow of “cold” ionospheric plasma with flow speeds  $\sim 8$  km/s for  $\text{O}_2^+$ . This flow would allow measurement of the lower ionosphere's composition. This polarization electric field  $\mathbf{E}_{\parallel} = -\nabla P_e / n_e$ , included in hybrid simulations shown later in the paper, verify that this ionospheric outflow can be an important loss term for the ionosphere and requires greater ion production from the exosphere than originally thought (note, such electric fields are included in the Lipatov et al., 2010 calculations).

At surface altitudes well above the possible “ionopause” the PUIs will dominate, the plasma flow will be non-zero and

correspondingly the convective electric field will be relatively large. Lipatov et al. (2010) showed asymmetric interaction along flanks with high speed flow  $\sim 180$  km/s on Europa's Jupiter side (West Longitude  $\lambda_W \sim 0^\circ$ ) where PUIs are directed downward and removed from the flow, while lower speeds  $\sim 100$  km/s on anti-Jupiter side ( $\lambda_W \sim 180^\circ$ ) are expected where PUIs move away from Europa and mass load the flow. Ignoring the finite-gyroradius effects generating such asymmetry, Schilling et al. (2008) compute a more symmetric interaction with their zero-gyroradius MHD approach. The directional sense of positive ion gyromotion is that PUIs moving upward to the spacecraft from below will be measured for  $90^\circ \leq \lambda_W \leq 270^\circ$ , while downward-moving PUIs from above reach the spacecraft at  $270^\circ \leq \lambda_W \leq 360^\circ$  and  $0^\circ \leq \lambda_W \leq 90^\circ$  west longitudes. The combination of upward moving PUIs and ionospheric outflows will provide the most direct information about the surface composition. For flow speeds  $\sim 100$  km/s the  $O_2^+$  PUIs are accelerated to energies  $\sim 100$ – $1000$  eV with gyroradii  $r_g \sim 60$  km; the maximum height of such ions, if born near surface, is  $\sim 2r_g$  or 120 km. With the spacecraft at  $\sim 100$  km altitude such medium-heavy ions can be detected, while lighter ions such as  $H_2O^+$  would need minimum altitude  $\sim 40$  km in order to be detected, and heavier ions such as  $CO_2^+$  could be detected at heights  $\sim 165$  km.

A simple fluid calculation shows that if the “local”  $O_2$  vertical column density is  $> 10^{15}$  mol/cm<sup>2</sup> the ionopause will be  $> 100$  km altitude and above orbiting spacecraft with altitude  $\sim 100$  km. If the column density is  $\leq 10^{15}$  mol/cm<sup>2</sup>, the ionopause height is below 100 km. When column densities are  $\sim 10^{14}$  mol/cm<sup>2</sup>, the convective electric field will extend down to the surface and allow IMS to probe PUIs forming near the surface and measure the heavier and more interesting exobiological molecules (i.e.,  $M/Q > 100$  amu). Heavy neutrals seeping through Europa's disrupted surface are likely to be very cold with  $T \sim 120$  °K and scale heights less than 20 km, as compared to spacecraft orbital altitude at least five times that distance, so detection as neutrals by INMS or NMS is unlikely. The pickup-ion approach may be the only way of detecting the heavier molecules of highest astrobiological interest.

### 1.5. Overall plan for determining Europa's intrinsic surface composition

Based on the introductory discussion above, our suggested overall plan for measuring Europa's intrinsic surface composition includes the following steps: (1) obtain a quantitative understanding of how logenic plasma is transported to Europa's orbital position, (2) understand the interaction of the moon with Jupiter's magnetosphere to determine what fraction of logenic plasma reaches the moon's surface and where, (3) use an IMS (with magnetometer) designed to work in Jupiter's harsh radiation environment with both major ion and minor ion detection capability and be able to separate  $O^+/S^{++}$  and  $O_2^+/S^+$  ions, (4) use the IMS to measure pickup ions from the body's exosphere to determine the surface composition, (5) utilize hybrid kinetic simulations of the interaction to determine height and thickness of the “ionopause”, if present, and to quantify how well this technique will work in terms of expected spatial resolution (i.e., the lower the “ionopause” relative to an orbiting spacecraft's altitude the better the technique will work). If the “ionopause” is above the spacecraft position but very thick on the ion gyroradius scale, the technique may still work with the magnetosphere's convective electric field extending down to the surface and (6) even if “ionopause” is below the spacecraft, field aligned outflows of the ionosphere over polar regions should allow measurement of the ionospheric composition.

### 1.6. Outline of paper

In the following sections of the paper we review properties of Jupiter's magnetosphere and the transport of logenic plasma to Europa (Section 2), Europa's  $O_2$  exosphere (Section 3), and radio science observations of Europa's ionosphere (Section 4). 3D hybrid simulations of Europa's interaction with Jupiter's magnetosphere are then described in Section 5 for the magnetic field and bulk plasma environment around Europa. Parameters from these simulations are compared to calculations of mass loading, ionopause height-thickness, and ionospheric ion temperatures and electron densities (Section 6). We then build on these results to compute predicted IMS PUI energy spectra (Section 7) and to model the measurement of surface composition from the PUIs (Section 8). In Section 9 we estimate ionosphere polar outflow, refilling rates, and exosphere consequences. Section 10 addresses other measurement issues and supporting measurements, followed finally (Section 11) by summary and conclusions.

## 2. Jupiter's magnetosphere and transport of iogenic plasma

The plasma within Jupiter's fast rotating magnetosphere is dominated by ionized neutrals injected into it by the Galilean moon Io having a surface covered with many active volcanoes (Smith et al., 1979; McEwen et al., 2006). The Voyager 1 and 2 encounters discovered the Io plasma torus which was dominated by oxygen and sulphur ions (Bridge et al., 1979a, 1979b; McNutt et al., 1981; Bagenal and Sullivan, 1981; Belcher, 1983; Broadfoot et al., 1979; Sandel et al., 1979). The Io plasma torus electron component was reported by Sittler and Strobel (1987). The full compositional range of iogenic elemental ion abundances would be characteristic of the solar system in an overall sense, but some abundances would vary in response to various fractionation processes, e.g., more volatile elements escaping in gaseous phase (Schaefer and Fegley, 2005a, 2005b) from volcanic plumes of Io to the torus while more refractory species would return to the surface. Sputtering from direct impact of energetic torus ions onto the Io surface, mainly through the thinner atmospheric layers on

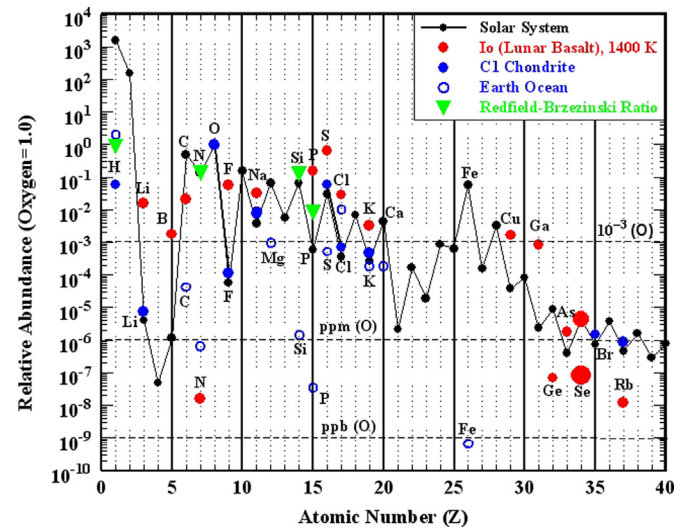


Fig. 1. Standard solar system abundances of elements H–Zr as compared to the very similar set for C1 Chondrites and to more variable abundances for Earth oceanic elements, biological materials in the Redfield–Brzezinski ratio (Brzezinski, 1985), and our new model by methods of Schaefer and Fegley (2005a, 2005b) for neutral volcanic gases from Io with the assumption of lunar basaltic composition within the source volcanic magma at Io. Although abundances are usually normalized to Si on Earth, we instead use predominantly abundant O at Europa as the reference element.

the nightside and the poles, might then become dominant torus sources of refractory elements.

Although some very important species, e.g., for determination of exact composition of iogenic vs. oceanic hydrate materials on Europa (Ca, Fe, Na, Mg, Si), are abundant relative to oxygen near the few percent (minor component) level, many others (e.g., Cl, K, P, Br, Rb, I, Cs) are at trace (ppm) levels as shown in Fig. 1 (see Dalton et al., 2010 on Europa surface composition by Galileo's Near Infrared Mapping Spectrometer (NIMS) imager). Note for example that N/O, P/O, Si/O, and Fe/O, respectively, vary by four to eight orders of magnitude from standard down to oceanic or iogenic abundances. Abundances of elements in the putative oceanic material potentially emerging to the sensible surface are unknown, and could for example be driven by hydrothermal inputs, salinity, oxidation state, and acidity (Zolotov and Shock, 2001, 2004; Pasek and Greenberg, 2012) but presumably fall somewhere in the range shown. Geochemical and astrobiological interest would be focused near Europa on the isotopes, which at least for major and minor species might be measurable at trace levels, e.g., the radiogenic isotope  $K^{40}$  at about 5 ppm relative to O. The least abundant but stable sulfur isotope  $S^{36}$  would be detectable at 600 ppm, thereby opening up the possibility of probing both Io magmatic and Europa oceanic processes through sulfur isotope fractionation. Heavier volatile isotopes would tend to accumulate at the moon surfaces, but lighter isotopes can escape via sublimation into the atmospheres and magnetospheres. Therefore, any hot spots of lighter isotopes in the astrobiologically significant elements (C, N, O, P, S, Ca, Si), including for oceanic biomineralization, could be indicative of active biological or prebiotic processes. Any organic remnants of life from the ocean would not survive for long in recognizable chemical form on the highly irradiated surface of Europa, but inorganic biomineral components would remain long after organic biosignatures had been destroyed by irradiation. Such components could be detectable as concentrations in oceanic surface emergence regions at scales from the elemental to microscopic and even macroscopic structural levels. Europa's surface abundance of Fe in emergent oceanic materials could be extremely informative, since this chemically active element is ubiquitous in solar system and terrestrial crust materials, had relatively high abundance in the prebiotic Archean oxygen-poor ocean of Earth, but, since the later evolution of the oxygen-rich atmosphere and cellular life, has had very low abundance in the highly oxidized modern ocean.

Krimigis et al. (1981), and later Mauk et al. (1996), found hot plasma dominated by heavy ions and this hot plasma dominated the plasma pressure of the magnetosphere for all the Galilean moons except for Io. This was later confirmed by Galileo Energetic Particle Detector (EPD) hot plasma ion composition observations by Mauk et al. (2004). The Galileo plasma instrument defined the plasma properties for various Europa flybys, including the first (E04) that came within 400 km of the surface (Paterson et al., 1999). In Kivelson's et al. (2009) Table 2 the cold and hot plasma properties of the magnetosphere are listed for the vicinity of Europa. Within the plasma sheet the value  $\beta \sim 0.5$  can occur for

the ratio  $\beta$  of plasma and magnetic field energy densities, while  $\beta < 0.1$  within lobe-like field lines. Near Europa the plasma flow velocity is  $V \sim 105$  km/s and, since Europa is moving  $\sim 13.7$  km/s in the same direction around Jupiter, the flow speed in Europa's frame is  $V \sim 90$  km/s.

Neither Voyager nor Galileo directly measured the composition of low-energy ions near Europa, but composition was inferred from the energy spectra and sonic Mach numbers of the measured flows. The mass resolution was highest when the plasma was cold and the sonic Mach number was largest such as inside Io's L shell (Belcher, 1983), while outside this L-shell the plasma was hotter and merged into a single peak in  $E/Q$ . Furthermore, the previous mission instruments could not separate  $O^+$  from  $S^{++}$ , so true measures of relative abundances for these two elementally different ions could not be made. Quantifying the transport of sulphur to Europa's surface from Jupiter's magnetosphere would provide a very important capability for a future mission to Jupiter's magnetosphere. An IMS with this capability would also better quantify the transport of iogenic plasma from the Io torus to all three icy Galilean moons. For Voyager plasma measurements (Belcher, 1983) at 8.6  $R_J$  the inferred composition was  $M/Q = (8, 16, 23, 32, 48, 64) \geq (28, 34, 0, 8, 0, 7)$  ion/cm<sup>3</sup>. These Voyager measurements gave mean  $\langle M/Q \rangle \sim 19$ , while Paterson et al. (1999) reported  $\langle M/Q \rangle \sim 12.5$  from the first (E04) flyby of Europa. So, there is much uncertainty in the  $\langle M/Q \rangle$  of the plasma, and larger values translate to greater dynamic pressures upon Europa's exosphere/ionosphere and greater likelihood of direct plasma penetration down to Europa's surface. Finally, within the plasma sheet where dynamic pressures are greatest for plasma  $\beta \sim 0.5$  and with hot ion gyroradii  $\sim 500$  km, one might indeed expect the penetration of the

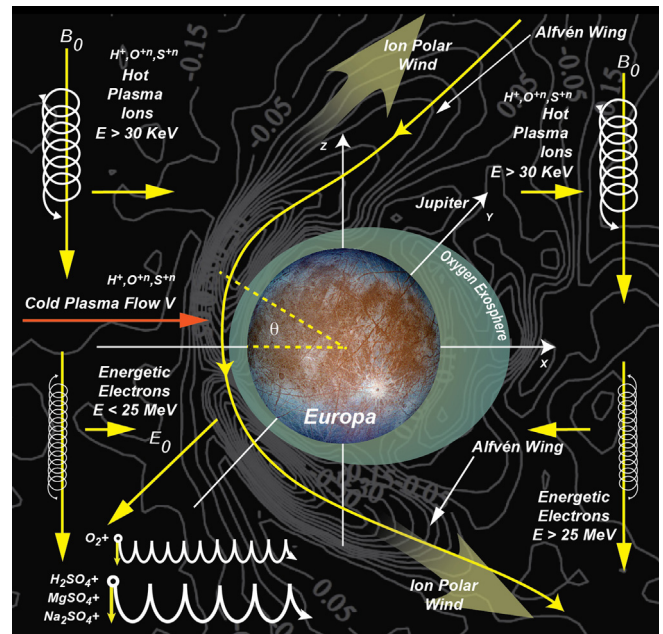


**Fig. 2.** Cartoon description of Europa with Jupiter's magnetosphere and definition of coordinate system for various simulations shown. It shows surface image of Europa, its darkened regions and numerous surface cracks. Intensity contours from Lipatov et al. (2010) model show electron flux and possible presence of polar field-aligned ion outflows driven by plasma electron produced field aligned electric fields. Draped field lines along Alfvén Wing are shown. Field lines then diffuse inside Europa's body which is not shown. Therefore, field aligned currents are expected and ion outflow will be sink to Europa's ionosphere. Figure also shows pickup ions with  $O_2^+$  dominating the pickup ion current which flow perpendicular to the magnetic field. Large gyro-radii hot plasma ions are shown along with their preferred direction of motion. The energetic electrons have smaller gyro-radii and move in corotation direction for  $E < 25$  MeV and in opposite direction for  $E > 25$  MeV (i.e., gradient-curvature drifts dominate over EXB flow).

**Table 2**  
O<sub>2</sub> atmosphere parameters and their authors.

Source	N1 (mol/cm <sup>3</sup> )	H1 (km)	Height range (km)	N2 mol/cm <sup>3</sup>	H2 (km)	Height range (km)
This paper	$5 \times 10^8$	20	All	NA	NA	NA
Cassidy et al. (2007)	$5 \times 10^8$	20	0 to 200	$5 \times 10^4$	500	$z > 200$
Schilling et al. (2008)	$1.7 \times 10^7$	145	All	NA	NA	NA
Lipatov et al. (2010)	$10^8$	20	0 to 200	$5 \times 10^4$	500	$z > 200$

magnetospheric plasma to Europa's surface, which would enable probing of the surface composition from PUI measurements at 100–200 km altitudes.

### 3. Europa's O<sub>2</sub> exosphere

The Space Telescope Imaging Spectrograph (STIS) of the Hubble Space Telescope (HST) observed atomic oxygen emission from Europa at 1304 and 1356 Å, which was attributed to an O<sub>2</sub> atmosphere by Hall et al. (1995, 1998). Fig. 2 shows cartoon of Europa's exosphere, its interaction with Jupiter's magnetosphere and the coordinate system used for our description of the interaction. As discussed in Cassidy et al. (2007), the O<sub>2</sub> atmosphere was predicted by Johnson et al. (1982) from magnetospheric plasma interaction with Europa's surface. The O<sub>2</sub> is made from energetic ion and electron bombardment of the icy surface and subsequent radiolytic decomposition of the water ice (Johnson, 1990). The 1304/1356 emission line intensity ratio suggested electron impact dissociation of O<sub>2</sub> and not impact excitation of atomic oxygen (Hall et al., 1995, 1998). The O<sub>2</sub> exosphere was found by Hall et al. (1995, 1998) to have vertical column densities for the trailing hemisphere  $\sim 2.4 \times 10^{14}$  to  $1.4 \times 10^{15}$  O<sub>2</sub>/cm<sup>2</sup>.

As determined by HST observations (McGrath et al., 2004), the O<sub>2</sub> atmosphere is patchy with brightest emissions over the Northern Bright Plains (NBP), where the surface is nearly pure ice, and weaker emissions elsewhere. Figs. 1 and 4 of Cassidy et al. (2007) showed HST/STIS 1356 Å images taken near dusk local time with a view of the trailing hemisphere at  $\sim 270^\circ$  west longitude. These figures showed super-imposed vertical O<sub>2</sub> column density contours with density maxima along the North Bright Planes  $\sim 200^\circ$  west longitude and  $\sim 45^\circ$  N latitude where PUIs would be moving away from Europa and mass loading on the local magnetic field lines would be most important.

The global distribution of O<sub>2</sub> in Europa's atmosphere presumably arises from distributed sources, such as the icy regions, but these molecules cannot in general be traced to unique surface sources. Cassidy et al. (2007) attempted to model the patchiness of the O<sub>2</sub> atmosphere by introducing a reactivity parameter such that  $R_{\text{eff}} \sim 0$  if no sticking occurs and  $R_{\text{eff}} \neq 0$  when sticking can occur (i.e., darker regions with SO<sub>2</sub> and CO<sub>2</sub> are sites where O<sub>2</sub> sticking can occur (Johnson et al., 2004; Hand et al., 2006)). For  $R_{\text{eff}} \sim 0$  the O<sub>2</sub> would tend to be absorbed and then desorbed many times before being lost via electron impact dissociation and/or ionization with time constants  $\sim 6$  days (i.e., long dissociation time scales allow O<sub>2</sub> molecules to move several thousand km around Europa before being lost to the surface). If  $R_{\text{eff}} > 0$  then O<sub>2</sub> molecules can stick in such regions, so one expects column densities to be lowest on the trailing hemisphere which has been darkened due to ion impact and radiolytic processes. Other molecules with  $R \gg R_{\text{eff}} \sim 0$  would have relative local surface sources and be traceable back to nearby points of origin. Since most O<sub>2</sub> comes from desorption it is in good thermal contact with the surface at temperatures  $T \sim 120^\circ\text{K}$  (Spencer et al., 1999) and thus has a scale height  $\sim 20$  km (Ip et al., 1998; Shematovich et al., 2005; Smyth and Marconi, 2006). Spencer et al. (1999) temperature maps from Galileo infrared measurements show  $T \sim 90^\circ\text{K}$  on the night side (leading side when at dusk LT and trailing side when at dawn LT) and very cold  $T \sim 40^\circ\text{K}$  at poles where O<sub>2</sub> emissions are very low (Cassidy et al., 2007). At the poles the convective electric field of the flow is tangential to the surface so PUIs are not readily lost to the surface and little attenuation in convective electric field is expected. See McGrath et al. (2009) for a more comprehensive review of the atmospheric observations. Other much heavier molecules of astrobiological interest would likely be in good thermal contact with the surface and have even shorter scale heights (Ip et al., 1998). These heavier

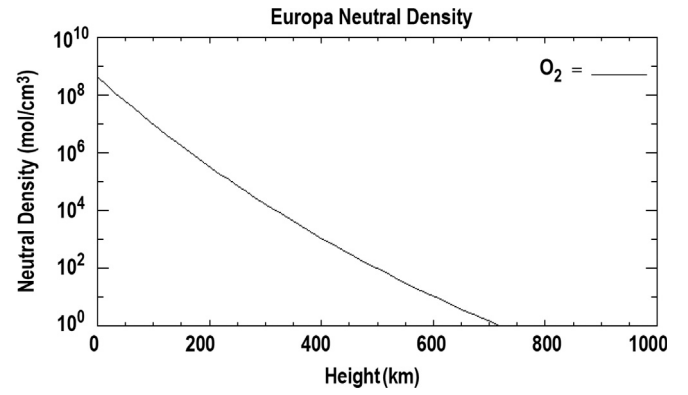


Fig. 3. Exosphere model of O<sub>2</sub> atmosphere.

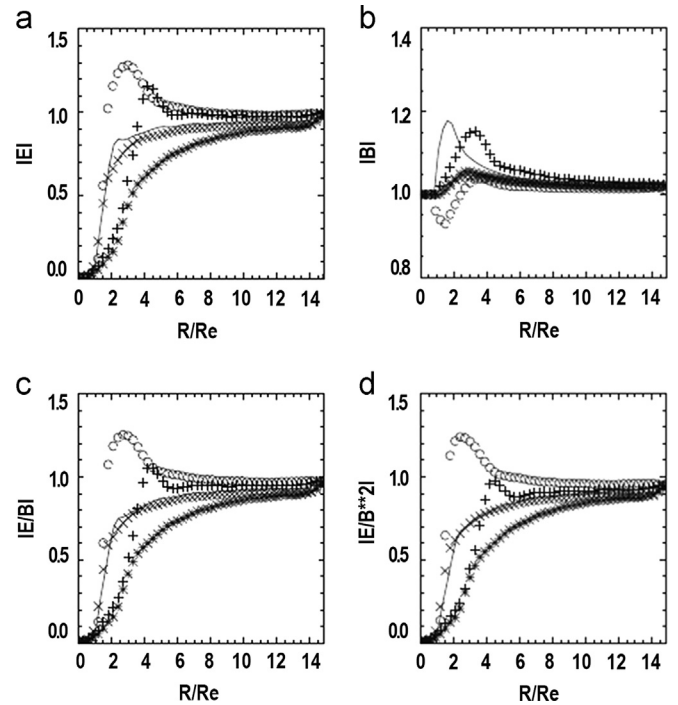


Fig. 4. Selected plots from Lipatov et al. (2010) paper. Radial cuts for  $|E|$ ,  $|B|$ ,  $|E|/B$  and  $|E|/B^2$ . Directions:  $-x$  (solid line),  $y(0)$ ,  $-y(+)$ ,  $z(*)$ ,  $-z(x)$ .

molecules would therefore not be observable at spacecraft altitudes as exospheric neutrals and would only be detected as PUIs.

In order to estimate realistic "ionopause" heights, one needs an exospheric model of the O<sub>2</sub> atmosphere, which is shown in Fig. 3. We used the exosphere model by Amsif et al. (1997) for parameters from Cassidy et al. (2007) with atmospheric temperature  $T \sim 120^\circ\text{K}$ , surface density  $N_{\text{O}_2} = 5 \times 10^8$  O<sub>2</sub>/cm<sup>3</sup> and scale height  $H_{\text{O}_2} = 20$  km. Column density is  $\sim 10^{15}$  O<sub>2</sub>/cm<sup>2</sup>. The exosphere calculation displays an increase in scale height with increasing radial distance or height with  $H_{\text{O}_2} \sim 20$  km near surface and  $\sim 32$  km at height  $z \sim 600$  km. Cassidy et al. (2007) do include a non-thermal component that becomes significant for heights  $z > 200$  km with  $N_{\text{O}_2} \sim 5 \times 10^4$  O<sub>2</sub>/cm<sup>3</sup>, but calculations show this component to have small effect on the mass loading of the flow (i.e., as shown in Fig. 7 do see a small large scale length slowing down at heights  $> 200$  km). Schilling et al. (2007, 2008) used a neutral density model with  $N_{\text{O}_2} \sim 1.7 \times 10^7$  O<sub>2</sub>/cm<sup>3</sup> with a scale height  $H_{\text{O}_2} \sim 145$  km and a column density  $\sim 5 \times 10^{14}$  O<sub>2</sub>/cm<sup>2</sup>. Their model uses Saur et al. (1998) assumption that O<sub>2</sub> column densities peak on trailing hemisphere where sputtering rates should

maximize and are minimum on leading or wake-side hemisphere for a trailing-leading density ratio of 2.3:1.

That Schilling et al. (2007, 2008) model the moon atmosphere with larger scale height is an indication that their 3D MHD model cannot resolve spatial scales  $<100$  km and therefore cannot resolve the “ionopause” boundary. Their simulations are more applicable to the large scale interaction at altitudes above 100 km. The hybrid kinetic model approach of Lipatov et al. (2010) fully account for finite gyro-radius effects ( $r_g \sim 30\text{--}500$  km) and uses  $N_{O_2} \sim 10^8$  mol/cm<sup>3</sup> near surface with scale height  $\sim 20$  km for heights  $\leq 200$  km and scale height  $\sim 500$  km for heights  $>200$  km, as done by Cassidy et al. (2007). In the first approximation Lipatov et al. (2010) assume uniform O<sub>2</sub> column density for all latitudes and longitudes. Their hybrid model also uses a multi-fluid approximation so it can compute field aligned electric fields  $E_{\parallel} \neq 0$  and thus ionospheric outflows driven by the polarization electric field. The Schilling et al. (2007, 2008) calculations are single fluid MHD and  $E_{\parallel} = 0$  is implicitly assumed. The O<sub>2</sub> neutral exosphere parameters used by various authors are summarized in our Table 2.

#### 4. Galileo radio science observations

The radio science (RS) observations by Kliore et al. (1997) during various Galileo flybys of Europa are very complex. A more complete set of RS results are given in McGrath et al. (2009). In some cases a “cold” ionosphere below 100 km altitude with an electron density  $n_e \sim 10^4$  el/cm<sup>3</sup> was observed. In other cases, no ionosphere was detected. For the first E04 flyby inbound an extended ionosphere  $\sim 500$  km was observed with  $n_e \sim 5000$  el/cm<sup>3</sup>. Uncertainties were large where electron densities  $\sim 5000$  el/cm<sup>3</sup> occurred. As we discuss below, the RS observations measured the electron column density along a line-of-sight (LOS) and Kliore et al. (1997) assumed a gravitationally bound spherical ionosphere with column density  $\sim \sqrt{2\pi R H n_e(R)}$ . For the E04 flyby the ionospheric scale height  $H \sim 250$  km for heights  $h \leq 300$  km and  $H \sim 440$  km for  $h > 300$  km.  $R$  is the radial distance or impact parameter of the tangential LOS, and  $n_e(R)$  is the electron density. If the true scale height  $H \sim 2R_E \sim 3000$  km, then the estimated density is  $\sim 30\%$  of the original estimate (i.e., spherical ionosphere may not apply).

Deflections of the flow can have important consequences for the inferred electron densities. For example, deflection of the flow toward Jupiter was reported (Paterson et al., 1999) during the E04 approach and after exiting the wake, while deflections toward the wake centre were observed at the wake boundaries. If so, the Galileo spacecraft was moving through the flanks of the interaction and a split tail exists as modelled in both Kabin et al. (1999) and Lipatov et al. (2010), then one might expect the RS experiment to observe an extended ionosphere with scale lengths of several thousand kilometers. Since this is what was observed, the true electron densities are lower than originally estimated. This is also seen for the later E6b flyby entry where the ionosphere peaks with  $N_e \sim 5000$  el/cm<sup>3</sup> at  $z \sim 100$  km with scale height  $\sim 100$  km. Here, the spacecraft is entering along the wake side of the flanks facing Jupiter where mass loading is not expected. In summary, one must interpret the inferred  $n_e$  with knowledge of the upstream flow properties and use a global interaction model like that developed by Lipatov et al. (2010).

#### 5. 3D hybrid simulations of Europa's interaction with Jupiter's magnetosphere

In Fig. 4 we show our previous 3D hybrid simulations of Europa's interaction with Jupiter's magnetosphere for the E04

flyby as modelled by Lipatov et al. (2010). The various panels show the convective electric field magnitude of the flow  $|\mathbf{E}|$ , the magnetic field magnitude  $|\mathbf{B}|$ , the plasma flow speed  $V = |\mathbf{E}/\mathbf{B}|$  and the ion gyro-radius  $r_g \propto |\mathbf{E}/\mathbf{B}|^2$ . The solid line corresponds to flow along the nose of the interaction, the circles correspond to flow along Jupiter's side of Europa or  $0^\circ$  west longitude, the + symbols correspond to the anti-Jupiter side or  $180^\circ$  west longitude, \* along north polar axis of flow and  $\times$  along south polar axis of the flow.

The magnetic field panel shows that the interaction penetrates down to the surface with effects on fields even inside the moon. This means magnetospheric plasma electrons  $T_e \sim 10$  eV can penetrate all the way down to the surface and dominate the ionization of Europa's surface-bound exosphere (Saur et al., 1998; McGrath et al., 2009). Along the nose of the interaction region a magnetic barrier forms at heights  $\sim 750$  km above the surface with amplitude  $\sim 20\%$  of the upstream field. On the sub-Jupiter side there is a depression in the field at similar heights while on the anti-Jupiter side there is  $\sim 20\%$  increase in  $B$  at heights  $\sim 2R_E$  above the surface due to pickup ion currents.

The panel for the flow speed  $V = |\mathbf{E}/\mathbf{B}|$  clearly shows the finite gyro-radius properties of the interaction. On the sub-Jupiter side, where pickup ions are directed downward and thus lost once formed, one sees an increase in the flow along the flanks similar to the MHD simulations by Schilling et al. (2008). But along the flanks on the anti-Jovian side, where pickup ions move away from Europa, one sees a decrease in the flow consistent with mass loading. This asymmetry is not displayed in the MHD simulations by Kabin et al. (1999) and Schilling et al. (2008) where a symmetric response is seen (i.e., ion gyro-radius  $r_g = 0$ ). The north pole experiences a decrease in the flow at higher altitudes relative to that appearing along the south polar axis. This north-south asymmetry in the plasma flow, controlled by the magnetic barrier and the Alfvén wing, can be traced to the oblique alignment of the incoming magnetic field and corresponding oblique orientation of the Alfvén wing and asymmetry in the magnetic barrier.

The panel for the ion gyro-radius shows significant decreases in the gyro-radius near the moon on the anti-Jupiter side, while on the sub-Jupiter side the reverse is seen. Along the nose and south polar axis the gyro-radii remain large near the surface. At  $180^\circ$  west longitude where mass loading dominates, the gyro-radii are smaller, so only very heavy ions with mass  $M/Q > 98$  amu/q (i.e.,  $H_2SO_4^+$ ,  $MgSO_4^+$ , and  $Na_2SO_4^+$   $\sim 98 \leq M/Q \leq 140$  amu/q) will have lines of origin down near the surface and be able to reach spacecraft altitudes  $\sim 100$  km. We do note that within the magnetospheric plasma sheet where  $B \sim 370$  nT the gyro-radii will be  $\sim 20\%$  larger. As shown in Hartle and Sittler (2007) and Hartle et al. (2011), these ions with  $\alpha = rg/H \gg 1$  will appear as ion beams coming from Europa's surface. Between  $180^\circ$  and  $270^\circ$  west longitude the gyro-radii will be larger and ions of lower mass born near the surface can be observed at spacecraft altitudes. Lighter ions can be observed but they must reside in higher altitudes of the exosphere. The more energetic and lighter sputtered neutrals,  $M/Q \sim 18$ , will be able to reach altitudes above 100 km. If these ions are formed near 100 km altitude the spatial resolution of the neutrals coming from the surface cannot be better determined than the formation altitude, e.g.,  $100 \text{ km} \times 100 \text{ km}$  in this case.

Finite gyro-radius effects and pickup ion currents can produce relatively large asymmetries in the interaction and underscore the importance of measuring the pickup ions with more ring-like velocity distribution functions (VDF) separate from the upstream ambient ions which are more likely to have Maxwellian VDFs. Such measurements should be compared to and extrapolated by multi-species hybrid simulations like that done by Lipatov et al. (2010), and would be essential for separation of plasma currents from ocean currents when probing Europa's sub-surface ocean using a magnetometer on an orbiting/flyby spacecraft. Therefore, a

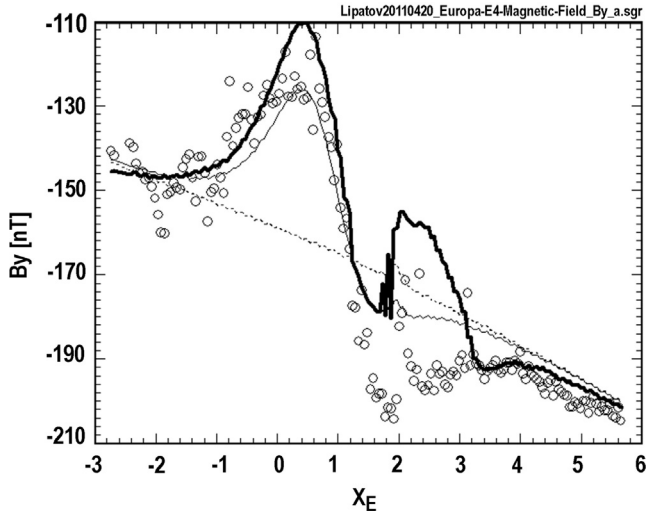


**Fig. 5.** Shows the  $B_y$  magnetic field component (components  $B_x$ ,  $B_z$ , and  $|B|$  not shown) along the E4 trajectory of the Galileo spacecraft after fitting with inductive dipole magnetic field (solid line). The circles denote the observational data. Simulation produces a satisfactory agreement with the observational data for the  $B_y$  magnetic field component. However, for the  $B_x$  and  $B_z$  magnetic field components an agreement is not so good yet. Probably one needs a multipole model for approximation of the ocean magnetic field.

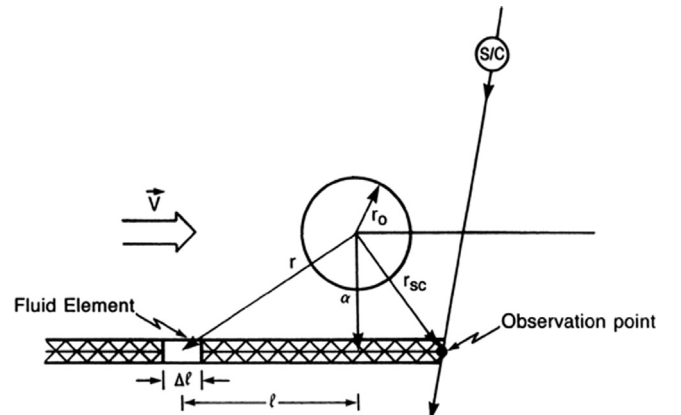
desirable feature of a plasma IMS on such a spacecraft, is the ability to separate ions within the instrument such as magnetospheric  $S^+$  ions and the pickup ions  $O_2^+$  which have nearly identical  $M/Q \sim 32$ . The  $O_2^+$  PUIs will be the ones dominating the dynamics while others such as  $H_2O^+$   $M/Q \sim 18$  are less likely to affect dynamics but would be important for other reasons such as measuring sputtering rates, and thus desirable to separate from the more dominant magnetospheric ions  $O^+/S^{++}$  with  $M/Q \sim 16$ .

Fig. 5 shows the  $B_y$  magnetic field observations for the E04 encounter and the corresponding simulated  $B_y$  values from the Lipatov et al. (2010) model calculations. In our hybrid kinetic modelling we first determine a simple dipole model of the induced oceanic magnetic field from the ten-hour corotation variation of the background Jovian magnetic field at Europa, perform the simulation for a fixed induced field and otherwise without a conduction ocean layer, and then fit the results of simulation for the components of the measured magnetic field. This is not yet a fully self-consistent approach but provides a first approximation. Also, the ocean may not be exactly a spherically symmetric conducting shell and may ultimately require a higher-order multiple model for the induced fields. The model results for  $B_y$  show a reasonable fit to the measurements near Europa but diverge significantly in the downstream, wake region where pickup ion effects become dominant. The same model gives less agreement to the  $B_x$  and  $B_z$  measurements, further highlighting the need to make full measurements of the plasma ion environment in support of oceanic induced magnetic field analysis. At  $X_E \sim 2-3$  the model produces a smaller secondary peak, which is also produced by Schilling et al. (2008) when induced oceanic current not included; the magnetometer data does not show this peak. When Schilling et al. (2008) add the induced oceanic currents the peak goes away with results very close to the magnetometer data. But Schilling et al. (2008) also do not get good agreement with  $B_z$  and  $B$  magnitude. We plan to use an induction model of the oceanic currents in the Lipatov et al. (2010) more in line with that used by Schilling et al. (2008) to resolve some of the discrepancies. If the models cannot yet fully reproduce the measured field components or the plasma moments, full field and plasma measurements are needed to better constrain model development in the future epochs of Europa missions.

Finally, these calculations have not yet included the hotter heavy plasma ions which can have gyroradii  $>500$  km, and penetrate down near the surface so the convective electric field caused by external flow may not be zero. This makes the observation of lighter pickup ions (i.e., smaller pickup gyro-radii since their max height will be  $z \sim 2R_g$ ) born down near the surface more likely. We are developing 2.5D (2D space and 3D in velocity) hybrid simulations so that improved spatial resolution  $\sim 30$  km can be achieved. This will allow us to resolve the “ionopause” and help answer important questions about PUI measurements at spacecraft altitudes  $\sim 100$  km and the ability of an orbiter to measure Europa’s surface composition, as will be the subject of future studies.

## 6. Mass loading calculation, ionopause location and ionopause thickness

Pressure balance between magnetospheric and planetary ionospheric plasma typically occurs by definition at the “ionopause” boundary, although this boundary is not well-defined for the surface-bound and largely collisionless atmospheric environment of Europa. In neither the MHD nor the hybrid cases do models resolve the “ionopause” layer but instead only the ionospheric region, at 80 km vertical resolution for the 3D MHD model by Schilling et al. (2008) at heights less than 750 km and at 150 km resolution for the 3D hybrid simulation by Lipatov et al. (2010). The advantage of the hybrid model is in providing a more accurate physical description of asymmetric PUI flows and magnetic background contributions on larger scales. In the future we will perform 2.5D hybrid simulations to achieve  $\sim 30$  km ionospheric resolution. A planned transformation of the 3D hybrid code to a composite grid structure including cubed-sphere geometry (e.g., Koldoba et al., 2002) for low altitudes will improve ionospheric resolution for the full computation. For now, one can perform two limiting cases with  $\sim$ km spatial resolution. The first is a fluid approach originally used for Saturn’s moon Titan by Sittler et al. (2005) and which neglects details of the interaction except for the mass loading effect. The fluid calculation implicitly assumes the ion gyro-radii are negligibly small, but does retain the effects of mass loading. The second approach by Hartle and Sittler (2007) and Hartle et al. (2011) does include finite gyro-radius effects but neglects mass loading effects, so this latter approach tends to under-estimate the ionospheric densities. The first is a 1D calculation, while the second applies to a 3D exosphere. The fluid approach indirectly gives ion temperature information, if one sets local ion temperature equal to the accumulated ion pickup energy



**Fig. 6.** Schematic of fluid mass loading calculation from Sittler et al. (2005) and used for our calculations shown in Fig. 7.

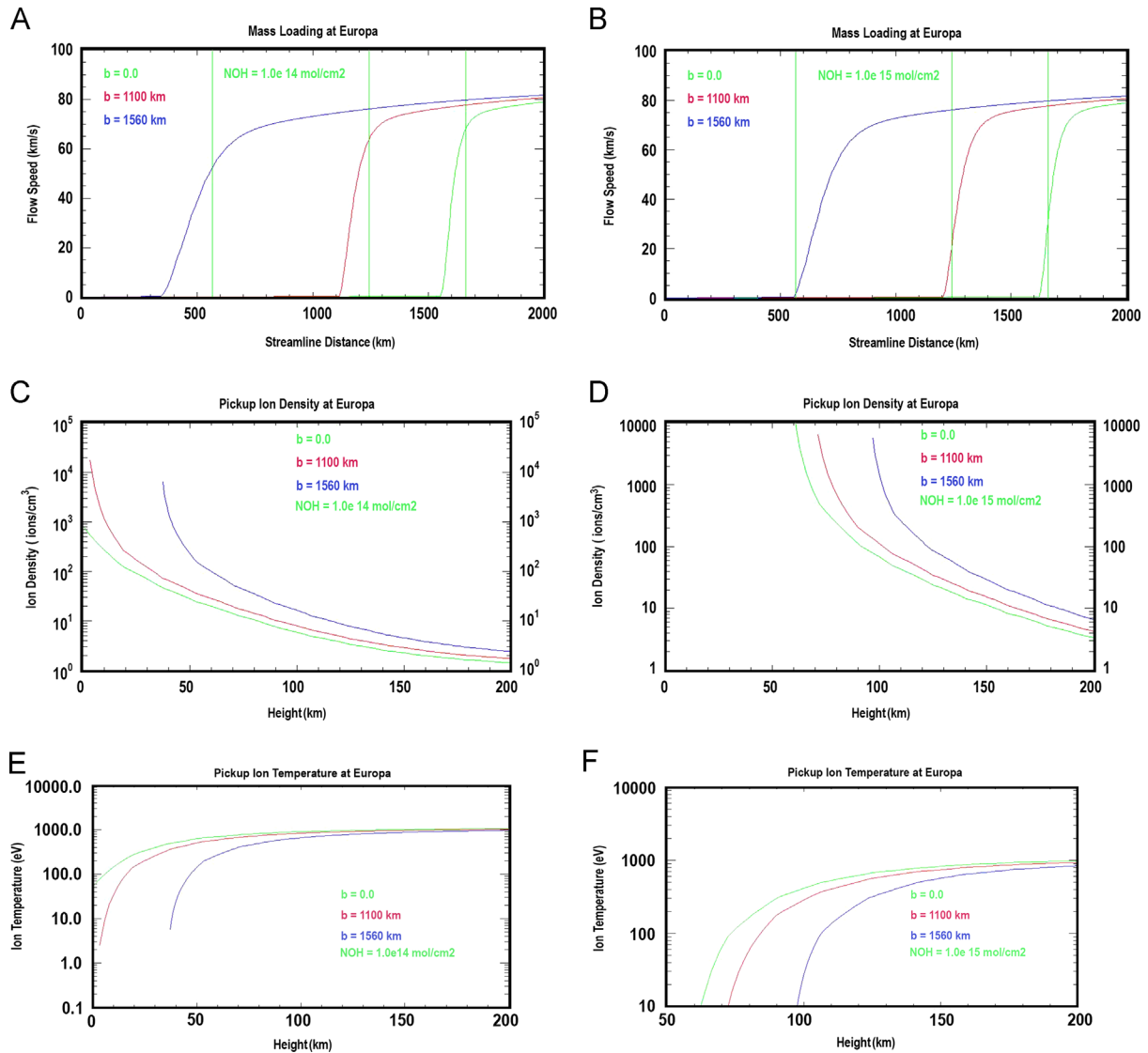


**Fig. 7.** Ionopause height calculated which includes mass loading from  $\text{O}_2$  exosphere. Vertical lines for panels A and B indicate spacecraft position at 100 km.  $b$  is impact parameter of upstream flow. Panel A is for low  $\text{O}_2$  column density of  $10^{14} \text{ mol/cm}^2$ . Panel B is for high  $\text{O}_2$  column density of  $10^{15} \text{ mol/cm}^2$ . Calculated pickup ion densities as function of height is given in panel C is for low  $\text{O}_2$  column density of  $10^{14} \text{ mol/cm}^2$  and panel D is for high  $\text{O}_2$  column density of  $10^{15} \text{ mol/cm}^2$ . In panel E is given pickup ion temperature as function of height for low  $\text{O}_2$  column density  $10^{14} \text{ mol/cm}^2$  and panel F is same but for high  $\text{O}_2$  column density  $10^{15} \text{ mol/cm}^2$ .

$T_{\text{ION}} \sim \Sigma 1/2(N_{\text{ION}}M_{\text{ION}}/k)v_{\text{PU}}^2/\Sigma N_{\text{ION}}$ , while the second approach will over-estimate the ion temperature and under-estimate the ion density. The first technique underestimates the ion temperature, since it neglects finite ion-gyro radius effects which tend to couple ions of different heights and west longitude. The correct solution should be somewhere in-between those of these two approaches. These solutions can be used to check the more complicated but physically more realistic 3D hybrid simulations by Lipatov et al. (2010).

For the fluid calculation of the “ionopause” boundary one uses the geometry shown in Fig. 6 from Sittler et al. (2005). The figure shows a fluid element moving along a straight line with impact parameter  $b$ . Flow along the ram axis of the interaction is indicated by  $b=0$  and will give the minimum height of the “ionopause” boundary. With  $b=R_E$  ( $R_E$ =Europa’s radius=1560 km) the flow is along the flanks of the interaction and tangentially grazes Europa’s surface. This calculation ignores deflections of the flow around Europa and, as stated previously, ignores finite gyro-radius effects. In addition to calculating the mass loading of the flow, this technique correctly calculates the PUI density within the fluid element (e.g., as the flow slows down, the fluid element has more

**Table 3**

Major and trace species in Europa’s exosphere (Cassidy et al., 2009).

Neutral type	Mass (amu)	$N(Z=0) \text{ \#/cm}^3$	$H \text{ (km)}$
$\text{H}_2$	2	$1.37 \times 10^6$	360
O	16	$1.28 \times 10^5$	400
OH	17	$1.16 \times 10^5$	400
$\text{H}_2\text{O}$	18	$2.57 \times 10^5$	400
Na	23	2000	400
$\text{O}_2$	32	$4 \times 10^8$ ; $5.4 \times 10^4$	24; 500
$\text{CO}_2$	44	$2.86 \times 10^4$ ; 27	20; 400
$\text{SO}_2$	64	$4.7 \times 10^5$ ; 296	15; 200

time to accumulate ions and electrons). The calculations use photoionization rates, electron impact ionization rates and charge exchange cross-sections (i.e., between the various components of the neutral exosphere such as H,  $\text{H}_2$ , O, OH,  $\text{H}_2\text{O}$ ,  $\text{O}_2$ , and their ions) as given in Sittler et al. (2005) and Smyth and Marconi (2006). Other than for  $\text{O}_2$  we obtained neutral gas densities and scale height from various references such as Cassidy et al. (2008), Smyth

**Table 4**

Ionization rates used for mass loading calculations and ion exosphere source terms from Sittler et al. (2004).

Reference	Type	Rate
Huebner and Giguere (1980)	$O_2 + h\nu \rightarrow O_2^+ + e^-$	$1.87 \times 10^{-8}$ ion/s
Huebner and Giguere (1980)	$O_2 + h\nu \rightarrow O + O^+ + e^-$	$1.94 \times 10^{-9}$ ions/s
Banks and Kockarts (1973)	$O_2 + e_{20 \text{ eV}} \rightarrow O_2^+ + 2e^-$	$4.35 \times 10^{-8}$ cm <sup>3</sup> /s
Banks and Kockarts (1973)	$O_2 + e_{100 \text{ eV}} \rightarrow O_2^+ + 2e^-$	$1.5 \times 10^{-7}$ cm <sup>3</sup> /s
Albritton et al. (1977)	$O_2 + O^+ \rightarrow O_2^+ + O$	$2.1 \times 10^{-9}$ cm <sup>3</sup> /s
Banks and Kockarts (1973)	$O_2 + O_2^+ \rightarrow O_2^+ + O_2$	$6.4 \times 10^{-9}$ cm <sup>3</sup> /s

and Marconi (2006) and other references. These constituents and their surface densities and scale heights are given in Table 3. The ionization rates and charge exchange rates are given in Table 4.

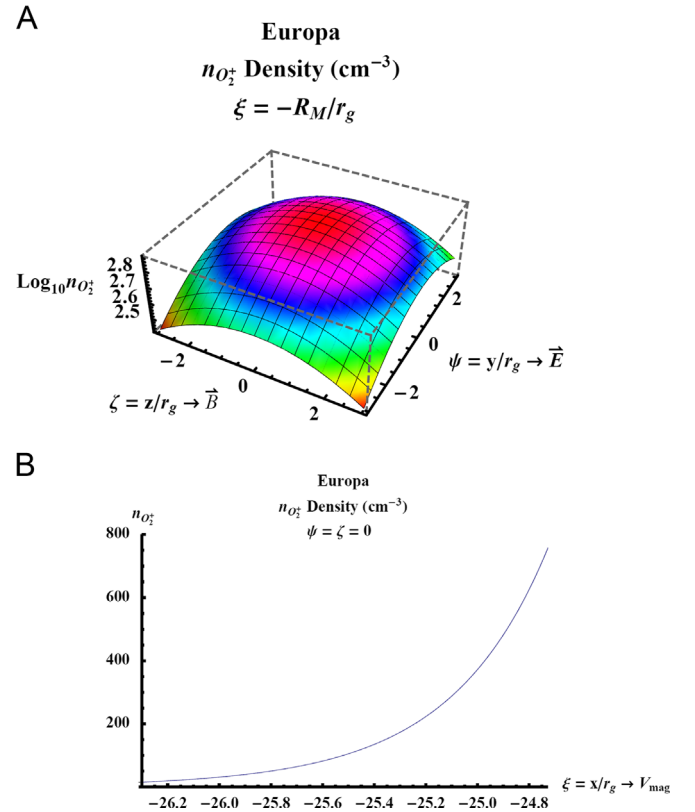
For the fluid calculation, we use two limiting cases with regard to an  $O_2$  atmosphere with spherical symmetry assumed. There is the low vertical column density limit for  $O_2$  of  $10^{14}$   $O_2$ /cm<sup>2</sup>, and the high vertical column density limit  $10^{15}$   $O_2$ /cm<sup>2</sup>. From Saur et al. (1998) and Schilling et al. (2007, 2008) the  $O_2$  neutral densities peaked on the trailing side of the moon where the magnetospheric plasma impacts the moon (i.e., nose of the interaction), while lower densities applied to the leading hemisphere or wake region. The rationale for this assumption was that sputtering rates would be higher on the trailing hemisphere. But, as discussed previously, Figs. 1 and 4 in Cassidy et al. (2007) and Figs. 4 and 5 in McGrath et al. (2009) showed lower column densities on the trailing side where the surface is darkened in the visible due to charged particle impacts and  $O_2$  molecules are more likely to react. Furthermore, higher  $O_2$  exosphere densities are favored on the anti-Jupiter side of the moon in the icy NBP region, where the mass loaded flank of the interaction is located and the surface is brighter for visible wavelengths (i.e., pure water ice and  $O_2$  is less likely to react, see discussions in McGrath et al. (2009)). Here, we note that the plasma interaction modelers such as Schilling et al. (2007, 2008) and Lipatov et al. (2010) use values intermediate between our two limits. If higher values are used the amplitude of the magnetic interaction tends to be too high and is inconsistent with Galileo magnetometer observations. Finally, our fluid calculations are terminated once the flow drops below 0.5 km/s.

Fig. 7 shows the slowing down of the flow for nose of the interaction,  $b=0$ , the flanks,  $b=1560$  km and an intermediate value  $b=1100$  km. The vertical green lines in Fig. 7 indicate the spacecraft altitude of 100 km for the three values of  $b$ . For column density  $10^{14}$   $O_2$ /cm<sup>2</sup>, Panel A, there is negligible slowing down of the flow at spacecraft altitudes for all impact parameters. It does show a slowing down of the flow near zero within an  $O_2$  scale height  $\sim 20$  km of the surface. In Panel C the electron densities can exceed  $10^4$  el/cm<sup>3</sup> near the surface similar to that found by Kliore et al. (1997) for heights  $<100$  km (i.e., E4 exit, E6a entry). In Panel E we show the estimated PUI temperature, which is  $T_{ION} \sim 1000$  eV at spacecraft altitudes and  $T_{ION} \sim 100$  eV down to one scale height of the surface. So, under these conditions the magnetospheric electric field can penetrate within a few scale heights of the surface and accelerate PUIs born near the surface up to the spacecraft where they can be observed by the IMS. For the upper column density limit  $\sim 10^{15}$   $O_2$ /cm<sup>2</sup>, panel B, the flow is stopped near spacecraft altitudes where the stagnated flow can produce a cold ionosphere when finite gyro-radius effects are ignored. Panel D shows that at spacecraft altitudes  $\sim 100$  km for  $b=0$ ,  $N_{ION} \sim 50$  ions/cm<sup>3</sup> and exceeds  $N_{ION} = 10^4$  ions/cm<sup>3</sup> for altitudes  $<60$  km. Panel F shows  $T_{ION} \sim 500$  eV for  $b=0$  and  $T_{ION} < 10$  eV for  $b=1560$  km (flanks) at spacecraft altitudes  $\sim 100$  km and  $T_{ION} < 10$  eV at 60 km altitude for  $b=0$ .

In reference to our Fig. 4 from Lipatov et al. (2010) the flow  $v \sim E/B$  on  $-x$  side (i.e., nose of interaction) looks similar to our Fig. 7A  $b=0$  solutions. On the anti-Jupiter side of Europa where

magnetospheric electric field points away from Jupiter, the cut in  $-y$ -direction of Lipatov et al. (2010) applies and looks similar to our Fig. 7A  $b=1560$  km flank solutions. In both cases there is an extended mass loaded slowing down of the flow. In contrast, on the Jupiter side of Europa, the  $+y$ -direction, the flow from the hybrid model increases along the flanks at higher altitudes before it decreases down near the surface, but this is not shown by our Fig. 7 solutions. On this side of Europa mass loading does not occur since PUIs are directed down to the surface and lost from the flow (i.e., finite gyro-radius effect). Schilling et al. (2008) MHD calculations show symmetric increase in flow along the flanks since finite gyro-radius effects are ignored. But, generally, the hybrid and MHD simulations cannot resolve the “ionopause”. Our solutions do show that the ionosphere at spacecraft altitudes will be fairly hot  $T_{ION} \sim 50\text{--}1000$  eV. IMS will be required to measure these ions and not a “classical” INMS.

In order to rectify the finite gyro-radius problem we make use of the calculations by Hartle and Sittler (2007) of pickup ions forming within externally flowing plasma that is impinging upon a 1D exponential exosphere. Here, we use a generalized form of that solution by Hartle et al. (2011), where the 1D exosphere is replaced by a spherical exosphere. For this model, the critical parameter is the ratio the PUI ion gyro-radius over the atmospheric scale height  $\alpha = r_g/H \sim 3$ . The only limitation of this calculation is that mass loading is not considered, so the amplitude of the ion densities and ion temperatures tends to be lower and higher, respectively, than actual values. In Fig. 8A we show a 3D plot of the  $O_2^+$  densities in  $(\zeta, \psi) = (z/r_g, y/r_g)$  for fixed value of  $\xi = x/r_g = -R_E/r_g$  (i.e., external flow moving in  $+x$  direction) in units of ion gyro-radius  $r_g \sim 63$  km



**Fig. 8.** Plots of Europa's hot  $O_2^+$  ion exosphere using formula presented in Hartle and Killen (2006), Hartle and Sittler (2007) and Hartle et al. (2011). Panel A is a 2D plot of the ion density on a plane  $(\psi, \zeta) = (0, 0)$  that intersects the surface at  $\xi = -R_E/r_g$ . In panel B we have a 1D cut along  $\xi$  with  $(\psi, \zeta) = (0, 0)$ . The surface is at  $\xi = -24.76 \sim -R_E/r_g$  with the spacecraft altitude  $\xi = (-R_E + 100 \text{ km})/r_g \sim -26.35$  which intersects ordinate axis with ion density  $\sim 10$  ion/cm<sup>3</sup>; at surface max density  $\sim 800$  ion/cm<sup>3</sup>. Near surface ion scale height  $\sim 21$  km, while at spacecraft altitudes  $\sim 30$  km.

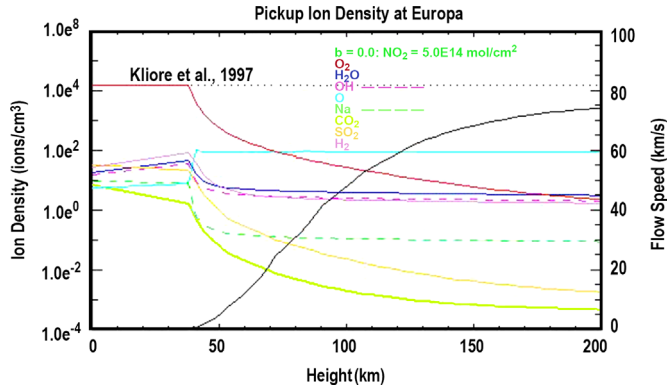


**Fig. 9.** Ion densities as a function of height from ionization of Europa's exosphere including the dominant component  $O_2^+$  and the minor species  $H_2^+$ , water group ions  $O^+$ ,  $OH^+$  and  $H_2O^+$  and ions  $Na^+$ ,  $SO_2^+$  and  $CO_2^+$ . The figure, right ordinate axis, also shows the flow speed (black line) of the plasma as it is mass loaded and eventually stops below 40 km altitude which is the ionopause. The  $O_2$  vertical column density assumed to be  $5 \times 10^{14}$  mol/cm<sup>2</sup>. These calculations assume zero gyro-radius.

for  $O_2^+$  PUIs. This solution corresponds to surface altitudes for  $(\zeta, \psi) = (0, 0)$ . In 8B we show 1D cut along  $\xi$  with  $\zeta = 0$  and  $\psi = 0$ . As can be seen, the scale height of the PUI ionosphere is much larger and more in line with the [Kliore et al. \(1997\)](#) observations. These solutions are close to the low column density case  $\sim 10^{14}$   $O_2$ /cm<sup>2</sup> PUI density and temperature plots in 7C and 7E, respectively for  $b = 0$ . The vertical tops of the PUI trajectories will be  $\sim 2r_g \sim 126$  km for  $O_2^+$ . Within the plasma sheet of the magnetosphere where  $B \sim 370$  nT, the  $O_2^+$  gyro-radii  $r_g \sim 78$  km and max altitude of trajectory will be  $2r_g \sim 156$  km. Estimated temperatures for this ionosphere are  $\sim 1100$  eV. Both sets of calculations when combined give strong evidence that the ionosphere observed by [Kliore et al. \(1997\)](#) is a hot ionosphere dominated by PUIs measurable by IMS and not a cold ionosphere that could be measured by INMS.

As discussed earlier, detection of minor species is an important goal of any future mission to Europa and the overall theme of habitability. Therefore, using the fluid calculations shown in [Fig. 7](#) the ion densities for more trace species as discussed in [Cassidy et al. \(2009\)](#) have been calculated and shown in [Fig. 9](#). These results used the neutral exosphere parameters given in [Table 3](#). We have done this for  $H_2$ , the water components ( $O$ ,  $OH$  and  $H_2O$ ),  $Na$ ,  $SO_2$  and  $CO_2$ . The calculations are based on cross-sections in [Sittler et al. \(2004, 2005\)](#), [Anicich \(1993\)](#), [Johnson et al. \(1998\)](#) and [Cassidy et al. \(2009\)](#). The  $O_2$  column density  $\sim 5 \times 10^{14}$   $O_2$ /cm<sup>2</sup> was assumed; left ordinate axis gives the ion density and right ordinate axis gives ion flow speed. As shown, the flow essentially stops below the "ionopause" with 40 km altitude. Once the flow has slowed to  $< 10$  km/s, all the electrons on a flux tube are removed from the interaction within one  $O_2$  scale height  $\sim 24$  km ( $\tau_e \sim 1$  s) of the "ionopause". Below 40 km altitude the approach by [Johnson et al. \(1998\)](#) is used, where electron impact ionization is negligible and one only includes photoionization of  $O_2$  and production of  $O_2^+$  from the charge exchange of the other ion species ( $H_2^+$ ,  $O^+$ ,  $OH^+$ ,  $H_2O^+$ ,  $Na^+$ ,  $SO_2^+$ ,  $CO_2^+$ ) with the  $O_2$  exosphere. One then sets the  $O_2^+$  to the max electron density observed by [Kliore et al. \(1997\)](#) which is  $\sim 1.5 \times 10^4$  el/cm<sup>3</sup> (very close to the  $O_2^+$  ion densities computed by the mass loading calculations when the flow stops (i.e., "ionopause")) and then using the relation  $N_{O_2^+}/\tau_L \sim N_{O_2}/\tau_i$  to solve for the ion convective loss timescale  $\tau_L$  with  $\tau_i$  the effective timescale for ionization of the  $O_2$  exosphere. This method yielded  $\tau_L \sim 1000$  s or effective flow speed to surface  $v \sim 40$  m/s. Then using this  $\tau_L$  one can estimate the ion densities as shown in [Fig. 9](#) for heights below 40 km; except for  $O^+$  which shows slight drop most of the ion densities jumped up into the range 10–100 ion/cm<sup>3</sup>. The  $O^+$  drops due to charge transfer losses with the  $O_2$  exosphere

(i.e.,  $O^+ + O_2 \rightarrow O + O_2^+$ ). Our ion densities are considerably lower than by [Johnson et al. \(1998\)](#) and likely due to considerable evolution of expected neutral densities in Europa's exosphere and the fact that our calculations take into account mass loading effects up to the "ionopause" which occurs in this case  $\sim 40$  km altitude. [Johnson et al. \(1998\)](#) calculations extend to  $> 200$  km altitude and therefore did not include upstream flow effects with mass loading (i.e., assumed stagnant ionosphere at all heights). Our calculations show that all the ion species will be observable for heights  $> 200$  km with IMS having ppm detection capabilities (i.e.,  $O^+$  upstream flow densities  $\sim 100$  ions/cm<sup>3</sup> so ppm  $\sim 10^{-4}$  ions/cm<sup>3</sup>). Finally, the caveat is made that finite gyro-radius effects could extend the flow down to near the surface, since this technique tends to over-estimate the mass loading.

So, in summary, our calculations show that the plasma flow can extend down near the surface for those cases when the  $O_2$  exosphere column density is  $< 10^{15}$   $O_2$ /cm<sup>2</sup>. The  $O_2$  exosphere is known to be patchy and have complex neutral density structures on the trailing side which can allow the flow along the nose of the interaction to extend down near the surface (see [Fig. 1](#) of [Cassidy et al. \(2007\)](#)). On the anti-Jupiter side,  $180^\circ$  west longitude, neutral density structures are complex but show higher neutral densities ([McGrath et al., 2009](#)). Therefore the combination of higher neutral densities and finite gyro-radius effects will make mass loading significant on this side of Europa. On the sub-Jupiter side neutral densities tend to be lower ([McGrath et al., 2009](#)), and flow speeds higher along the flanks (i.e., PUIs directed down to surface), so no mass loading on this side of Europa is expected. Here, the spacecraft will be observing pickup ions born at higher altitudes and composition dominated by lighter ions. It was also shown that ion temperatures would generally be between 50 and 1000 eV within the pickup regions and that trace ion densities  $H_2^+$ ,  $O^+$ ,  $OH^+$ ,  $H_2O^+$ ,  $Na^+$ ,  $SO_2^+$ ,  $CO_2^+$  below the "ionopause" were estimated to be  $\sim 10$ – $100$  ions/cm<sup>3</sup> and be detectable beyond 200 km altitude by IMS with ppm capability. Field-aligned outflows will tend to enhance the detectability of these ions at altitudes  $> 100$  km.

## 7. Predicted IMS energy spectra of pickup ions

In this section we compute the predicted energy spectrum for pickup ions that would be observed by the IMS on spacecraft in equatorial orbit around Europa (note equatorial orbit used for convenience) with a spherical exponential exosphere. We use the formula derived in [Hartle and Sittler \(2007\)](#) and [Hartle et al. \(2011\)](#) and the equation of PUI origins as given in [Hartle and Killen \(2006\)](#). [Fig. 10](#) shows the geometry used to compute PUI origins

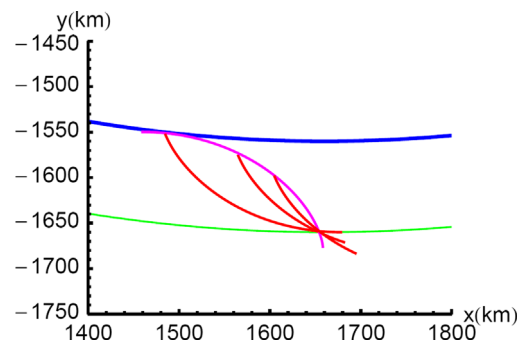


**Fig. 10.** Shows geometry used to compute pickup ion intensities as a function of energy shown in [Fig. 11](#). It shows line of origins for  $O_2^+$  pickup ions assuming constant  $E = -V \times B$  electric field pointing radially away from the moon's surface. External flow speed  $V \sim 85$  km/s and external magnetic field  $B \sim 450$  nT.

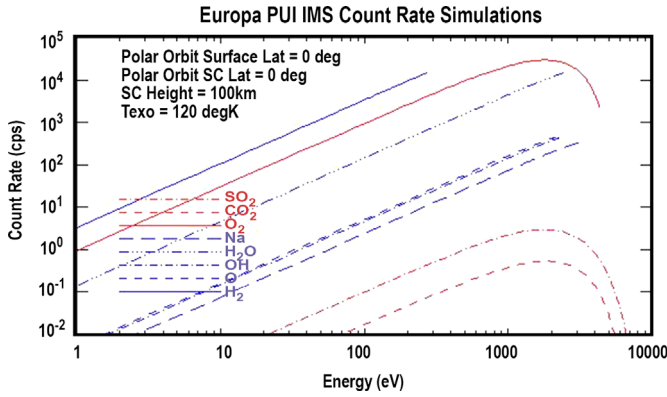


**Fig. 11.** Simulated energy spectrum that could be observed by IMS. It shows ion count rates for pickup ions using geometry shown in Fig. 10. For convenience an equatorial orbit of 100 km altitude is assumed for the spacecraft. IMS GF  $\sim 10^{-4}$  cm<sup>2</sup>-ster-eV/eV is used. Angular dependence not considered. Used formulae in Hartle and Sittler (2007) and Hartle et al. (2011).

with PUI trajectories superimposed.

$$x_0 = x_c - r_g(p + \sin p) \quad (1)$$

$$y_0 = y_c + r_g(1 - \cos(p)) \quad (2)$$

with  $x_c = 1260$  km,  $y_c = -1531$  km,  $r_g = MV_b/(eB)$  is the pickup ion gyro-radius,  $M$ =ion mass,  $e$ =electric charge,  $V_b = 85$  km/s is the upstream flow speed in the  $x$ -direction,  $B = 450$  nT is the upstream magnetic field and  $r_E = 1560$  km is radius of Europa. The min altitude of the PUIs is at the surface (i.e.,  $r = \sqrt{(x_0 - r_E)^2 + y_0^2} = r_E$ ).

The parameter  $p=0$  at the lowest altitude source point and  $p=-\pi$  is at the spacecraft position. We then varied  $p$  to adjust the point of origins from which the PUI energy can be calculated at the spacecraft position as described in Hartle and Sittler (2007).

$$v_x = V_b(1 - \cos p) \quad (3)$$

$$v_y = V_b \sin p \quad (4)$$

The ionization rates for the different ion species are given in Table 4. The results are shown in Fig. 11. The instruments geometric factor, the effective surface area of electrostatic analyzer (ESA) entrance system is GF  $\sim 10^{-4}$  cm<sup>2</sup>-ster-eV/eV (per angular sector). Even though H<sub>2</sub> is less abundant than O<sub>2</sub> their predicted signal is higher, since there are contributions over many origin sites due to its much smaller gyro-radius with  $\alpha < 1$  (i.e., sampling many PUI trajectories). The O<sub>2</sub><sup>+</sup> peaks at 2 keV and turns over at higher energies as the site of origin moves to higher altitudes in Europa's exosphere. The peak gives the minimum altitude of the PUI site of origin and nearest to the surface. As Fig. 10 shows the ions of different energy will also have different arrival directions. Since a coincidence detection system with sufficient shielding of detectors will be used, coincidence count rates less than 1 Hz are possible, in this case for CO<sub>2</sub><sup>+</sup> and SO<sub>2</sub><sup>+</sup>. The figure shows that the heavier ion count rate peaks at higher energies. It is also clear from this figure that one needs an IMS to separate the different ion species at the same  $E/Q$ . These estimates are based on model projections and only representative of what would be observable (see Cassidy et al., 2009).

## 8. Measurement of surface composition from pickup ions

The measurement approach is to alternate between times measuring pickup ions and times measuring plasma and magnetic field parameters along the spacecraft trajectory. By measuring the pickup ion energy, arrival direction and mass-per-charge, the ion can be traced back along the ejection trajectory to the approximate

area of origin if the 3-D electric field and magnetic field are known. *In situ* observations of plasma flow velocities and vector magnetic fields can be used to determine the local convective electric field ( $\mathbf{E} = -\mathbf{V} \times \mathbf{B}$ ) along the spacecraft trajectory. In addition, the IMS will provide the dynamic ram pressure by also measuring the mass density of the flow, while the IES will measure the hot ion pressure. By combining these pieces of information with models of the magnetospheric interaction with Europa (Lipatov et al., 2010), properly accounting for the ocean induced magnetic fields (Schilling et al., 2007, 2008), one can generate 3D maps of the electric and magnetic field and compute the trajectories of the pickup ions as test particles back to the surface or exospheric points of origin. With this combination of plasma measurements, magnetometer measurements and 3D models of the interaction one can make corrections to the magnetometer measurements of the induced oceanic magnetic fields.

The proposed technique can only sample ions above the "ionopause" where the magnetospheric electric field can penetrate and accelerate the newly born ions up to the spacecraft position where they can be observed. When the ion gyro-radius is  $R_g > 1/2$  the spacecraft altitude of 100 km (see Hartle and Sittler, 2007), these ions can be traced down to the moon's surface if the "ionopause" penetrates to such depths (i.e., O<sub>2</sub> vertical column density regions  $< 10^{15}$  mol/cm<sup>2</sup>). If the "ionopause" altitude is above the surface one can use the observed energy spectrum of the pickup ions to approximately determine the points of origin down near the surface. Assuming the observed ion spectrum is primarily due to PUIs, then If a local peak is present in this spectrum, one can use the peak's width to get approximate estimate of the neutral atmospheric scale height, the peak position to infer the PUI ion gyro-radius, and then trace trajectories to approximate points of origin near the surface (i.e., a narrow peak indicates small scale height relative to the ion gyro-radius or  $\alpha = R_g/H \gg 1$  (Hartle and Sittler, 2007) which is true for O<sub>2</sub>). As noted in Cassidy et al. (2007), species with high effecting sticking coefficients such as H<sub>2</sub>O, H<sub>2</sub>O<sub>2</sub> and Na will not travel far from their source points, although their higher sputter velocities will tend to spread them out spatially. Therefore, spatial maps with resolutions  $\sim 100$  km  $\times$  100 km are also possible for these species. In reality the picture is more complex and a 3D hybrid code is needed to construct more realistic 3D maps of the electric and magnetic fields. One can then use regions of known composition from imaging spectrometers to calibrate the technique and thus the global 3D electric and magnetic fields which can then be used to measure and map to the surface of more minor species that the imagers cannot hope to detect.

## 9. Ionosphere polar outflow, refilling rates and exosphere consequences

The IMS can measure a polar outflow of the ionospheric plasma as shown in Fig. 12 by our earlier hybrid kinetic simulations (see Lipatov et al., 2010). These outflows can also give information about ion composition near Europa's surface. Fig. 12 shows electron intensities in  $x$ - $y$  and  $x$ - $z$  projections. It shows intensification at nose of the interaction ( $b=0$ ) and along field lines (i.e., Alfvén wings). The intensification which decreases along field lines away from Europa forms parallel electric field  $E_{\parallel} \neq 0$  and an associated field aligned polar wind. One can estimate the ionospheric outflow using the following approach which can then be compared with the kinetic results shown in Fig. 12. For ionospheric  $T_e \sim 10$  eV (Saur et al., 1998), electron scale height  $H_e \sim 250$  km (Kliore et al., 1997) one can derive field aligned polarization electric field  $eE \sim -kT_e \nabla \log(n_e) \sim -kT_e/H_e \sim 77$  times force of gravity for O<sub>2</sub><sup>+</sup> ions. This can lead to ionospheric polar outflows  $\sim 8$  km/s (north and south) that can

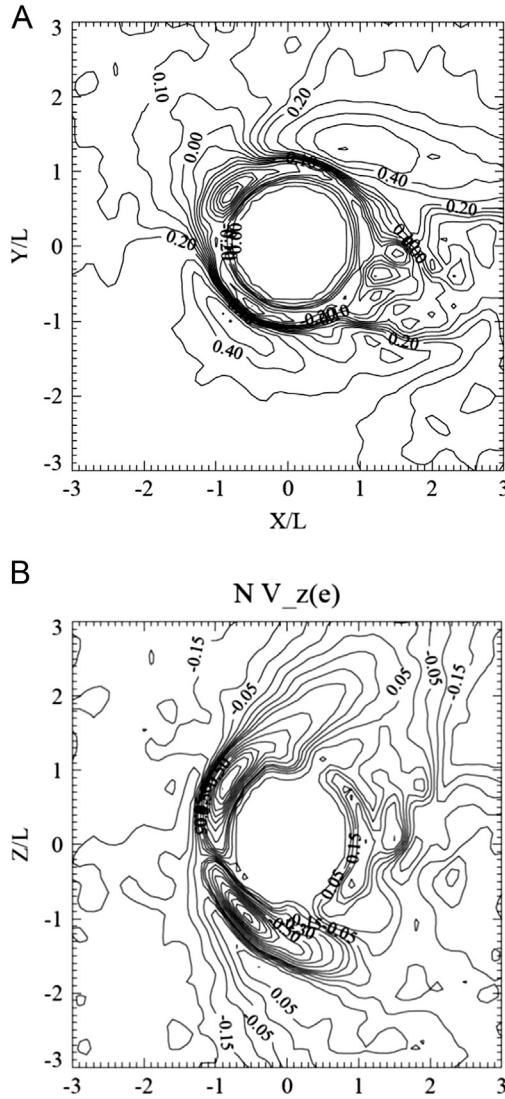


**Fig. 12.** Shows electron intensities derived from model by Lipatov et al. (2010). Intensities given in  $x$ - $y$  and  $x$ - $z$  planes. Panel A shows intensities peaking around nose of interaction and extending around to the flanks. Panel B shows field-aligned gradient (i.e., Alfvén wings) where field aligned outflows are computed. Significant ion outflows are computed and must be supported by the ionization of the exosphere. The extension of the contours below Europa's surface is caused by the average over the grid cells near Europa's surface (i.e., spatial resolution  $\sim 170$  km).

be measured by the IMS. This outflow is estimated to be  $\sim 10^9$   $\text{O}_2^+$  ions/ $\text{cm}^2/\text{s}$ . Assuming field aligned column density  $\sim \pi R_e n_e \sim \pi (1560 \text{ km})(1000 \text{ el}/\text{cm}^3)(10^5 \text{ cm}/\text{km}) \sim 4.9 \times 10^{11} \text{ el}/\text{cm}^2$  one can estimate refilling time scales  $\sim 4.9 \times 10^{11} / 2.0 \times 10^9 \text{ s} \sim 245 \text{ s} \sim 4 \text{ min}$ , which is comparable to the timescale it takes the plasma to convect past Europa. The outflow provides an important sink for the ionosphere. Therefore, the ionosphere should not have enough time to equilibrate with the exosphere and/or surface and thus should be hot with field-aligned  $T_{\text{ION}} \sim 10$ – $100$  eV for out flowing ionospheric plasma. This further reinforces our view that an IMS is required to measure the ionospheric ions.

## 10. Other measurement issues and supporting measurements

Here, we discuss other measurement techniques that could be used to support the proposed payload in Table 1. Ganymede observations are briefly mentioned due to ESA's JUICE (Jupiter

Icy moons Explorer) mission with Ganymede as the prime target. This mission also has two flybys of Europa with heights  $\sim 400$  km from Europa. Since the radiation environment is very challenging for a Europa orbiter mission, we also discuss possible radiation measurements that the spacecraft could provide.

One of the measurement techniques often discussed for a Europa orbiter mission is the Langmuir Probe (LP) which measures the electron density and electron temperature for energies below 40 eV and ion currents below 40 V. Ion ram energies in the Europa environment will generally be above 50–1000 eV so the ion current will essentially be a dc current except for light ions like  $\text{H}^+$ . Referring to Sittler and Strobel (1987), one can show that in the vicinity of Europa more than half of the electron current into the LP is carried by the hot electrons for  $E > 100$  eV, so current variations in the LP can be caused by electrons not directly measured by the LP. It is noteworthy that the hot electrons can dominate the electron pressure. One can use a dual LP technique (see Pedersen et al., 1998, Maynard, 1998 and Bale et al., 2008) to measure convective electric fields which are below 45 mV/m ( $\mathbf{E} = -\mathbf{V} \times \mathbf{B}$ ) at Europa. This technique can measure the plasma flow velocity  $\mathbf{V}_\perp$  perpendicular to the magnetic field, but it can only measure  $\mathbf{E}_\perp$  projected along the boom axis which introduces some ambiguity. These electric field measurements can be difficult since spacecraft charging fields can be  $\sim 1$ – $10$  V/m for  $r < 1$  m from spacecraft surface with plasma Debye length  $\lambda_D \sim 10 \sqrt{T_e(\text{eV})/n_e(\#/\text{cm}^3)} \text{ m} \sim 3$  m (i.e.,  $> 10$  m booms tip-tip will be required and at least three booms to measure all three components of the electric field). To measure  $E_{\parallel} \sim 40 \mu\text{V}/\text{m}$  with a LP would be very challenging but alternatively very straight-forward for an IMS. The same can be said for convective flows. The spacecraft itself can be a noisy environment (see Blackburn et al., 2011) and wake effects (Lipatov et al., 2012; Ergun et al., 2010; Maynard, 1998) can further complicate the spacecraft induced electric fields to make these dc measurements very difficult. In Sittler and Strobel (1987) one sees wide swings in spacecraft potential from positive to negative values in the vicinity of Europa which will further complicate the LP measurements. Finally, only the IMS can measure the mass density of the flow and thus the dynamic ram pressure of the flow, the IES is needed to measure the hot plasma pressure with temperatures of several hundred keV (Mauk et al., 2004), and the ELS is needed to measure field aligned currents ( $\mathbf{E}_\parallel$ ) and electron ionization rates with cross-sections that peak  $> 100$  eV electron energy. Sittler and Strobel (1987) show that more than half of the ionization rate of neutrals and ions in the vicinity of Europa are produced by the hot  $T_H \sim 250$  eV electrons which cannot be measured by the LP. A LP may provide complementary observations for the IMS primarily for low frequency plasma waves and dc electric fields if antennas are sufficiently long  $\sim 10$  m tip-to-tip. These antennas could provide measurements of the electron density and electron temperature primarily in cold dense ionosphere environments occurring in the ionospheres of Europa, Ganymede and Callisto. But, ion measurements of the magnetosphere and icy moon ionospheres must be done by the IMS and IES. ELS would provide the same measurements over a much wider range of electron energies (1 eV to 30 keV), unless the ionospheric electrons are relatively dense  $n_e > 100 \text{ el}/\text{cm}^3$  and very cold with  $T_e < 1$  eV. If the spacecraft potential  $\phi_{\text{SC}}$  is negative, then IMS measurements of  $\text{H}^+$  energy shift relative to the heavy ions  $\text{O}^+/\text{S}^{++}$  flow speed can be used to estimate  $\phi_{\text{SC}}$ , which can then be used to estimate the electron density from the ELS measurements (see Sittler et al., 2006).

In the case of Ganymede its internal magnetic field complicates the analysis. Galileo observations do show evidence of a polar wind (Kivelson et al., 2006) wherein the field lines are open so one could infer surface composition in the polar regions by measuring

the polar wind composition (i.e., same can be done for Europa). This polar wind was first reported [Frank et al. \(1997\)](#) as proton outflows, but later [Vasyliunas and Eviatar \(2000\)](#) and [Eviatar et al. \(2001\)](#) interpreted the polar wind ions as atomic oxygen ions from Ganymede's ionosphere. The plasma data also shows that the heavy ions of the Jovian magnetosphere are excluded from the Ganymede magnetosphere ([Kivelson et al., 2006](#)). [Williams et al. \(1998\)](#) showed drop in loss cone fluxes of energetic particles after they have mirrored near Ganymede's surface (i.e., G2 polar pass). [Cooper et al. \(2001\)](#) performed a particle trajectory analysis to show that penetration of magnetospheric particles inside the closed field region would be reduced orders of magnitude by dipolar magnetic deflection. For analysis of Ganymede observations one must construct 3D MHD or Hybrid models of the magnetospheric interaction with Jupiter's magnetosphere since transport time scales can be relatively short ~1 h or less and polar cap transport of ionospheric plasma can become mixed with a return flow of Jovian magnetospheric plasma from Ganymede's magnetic tail and thus complicate the surface composition measurements near equatorial latitudes.

Due to the high radiation environment, an array of dosimeters ([Hammock et al. 2009a, 2009b](#)) should be used to monitor the radiation environment. This can be used as a reference for background changes within various instrumentation and perform a health and safety role for the spacecraft and science payload if anomalies develop. This can assist in assessing instrument performance and the implementation of background corrections as needed. The radiation environment around Europa, as seen by an orbiting spacecraft, would vary along the orbit from highest fluxes on the trailing hemisphere to lowest on the leading hemisphere ([Paranicus et al., 2009](#)). Smaller scale variations may occur in association with boundary regions of compressed or relaxed magnetic field. Since these variations cannot always be predicted from models, the dosimeter array would allow the spacecraft to sense and make real-time decisions about impacts of increased or decreased fluxes on spacecraft and instrument operations. The dosimeters can also be used to validate and extrapolate from models for all points along the orbit. Dosimeter rates can be compared to instrument background channel rates to check on efficiency of background rejection.

## 11. Summary and conclusions

In this paper we have reviewed the Voyager and Galilean observations relevant to Europa's interaction with the Jovian magnetosphere and put in context with a hybrid simulation of the interaction as first reported by [Lipatov et al. \(2010\)](#). We have also provided simulations of the "ionopause" location relative to spacecraft orbital heights ~100–200 km that cannot be resolved by the Hybrid model or MHD models and the in situ observational implications this layer provides. Surface composition can be directly measured if the "ionopause" height is near the surface, while if above the spacecraft in situ measurements of pickup ions can give a more global description of the surface composition. We present arguments that ion gyro-radius effects could make the "ionopause" relatively thick and allow convective electric fields from the external flow to extend down near the surface even if it resides above the spacecraft location with height ~100 km. Model results also show that polar outflows of the ionosphere can be used to measure the composition of the ionosphere below spacecraft heights. From this modeling one can make a recommended in situ instrument suite (see [Table 1](#)) for both characterizing the sub-surface ocean and measuring the surface composition (i.e., magnetometer plus in situ plasma observations). From the proposed in situ instrument suite we presented measurement

techniques using an IMS, such as now being developed by us under the NASA Astrobiology Instrument Development Program (ASTID), with the first goal to measure the plasma interaction (i.e., measure dominant ions) between Jupiter's magnetosphere and its moons Europa, Io, Ganymede and Callisto. In the case of Europa this technique will support the magnetometer's detection of its sub-surface ocean as previously discussed. The second goal is to constrain composition, chemistry and space weather effects on the surfaces of the moons Europa, Ganymede and Callisto. Europa's surface composition includes potentially large contributions from Io torus plasma ( $O^{++}/S^{+4}$ ,  $S^{+3}$ ,  $O^{+}/S^{++}$ ,  $Na^{+}$ ,  $S^{+}$ ,  $K^{+}$ ,  $SO_2^{+}$ , etc.) transported out to Europa's L shell and then implanted onto the surface and material extruding from its sub-surface ocean to the surface ([Doggett et al., 2009](#)). It is known from Galileo Near Infrared Mapping Spectrometer (NIMS) observations that this material can be sulfate salts such as  $H_2SO_4^{+}$ ,  $MgSO_4^{+}$ , and  $Na_2SO_4^{+}$  ([Carlson et al., 2009](#)). But, does the sulfur come from Io or from the ocean? It is felt that hydrate sulfates are due to exogenic sulfur from Io, while magnesium sulfates have endogenic origins from Europa ([Dalton et al., 2010](#)). If from the sub-surface ocean, do the associated sulfate salts contribute to its conductivity ([Khurana et al., 2009](#)) and/or contribute to biochemistry for any micro-organisms in the ocean ([Hand et al., 2009](#))? Answers to these questions are fundamentally important to NASA, ESA, and the international astrobiology community. The goal of detecting minor species is achieved by measuring pickup ions at spacecraft altitudes. The pickup ion measurements are traced back to surface source regions using measurements of the upstream flow (IMS, IES, ELS; dominant ions) and a 3D hybrid model of the interactions to construct a global model of the electric and magnetic fields around these bodies. In the case of Europa we also show that Europa's ionosphere is dominated by pickup ions with 50–1000 eV temperatures. Excursions to a "classical" cold ionosphere for the INMS at spacecraft altitudes ~100 km are expected to be infrequent.

Finally, NMS observations and neutral exosphere models could additionally provide independent estimates of production rates of pickup ions since the IMS only measures the products of atmospheric ionization and pickup in the magnetospheric field. The hot plasma ion measurements are needed to correct for sputtering rates which can be time dependent, while electron plasma observations are needed to compute electron impact ionization rates. Also, as noted numerous times, the hot plasma measurements are important since the hot ion plasma dominates the magnetospheric pressure at Europa, Ganymede and Callisto, and the plasma electron observations provide information about parallel electric fields which can produce field-aligned ion outflows from the moon ionospheres. Such outflows can be an important sink for the ionospheres and result in lower ionospheric densities than otherwise thought. We conclude by listing suggested plasma instrument requirements in [Table 1](#) for future missions to Europa, Ganymede, and the Jupiter magnetosphere.

## Acknowledgements

This work has been supported under the NASA Astrobiology Instrument Development (ASTID) and Outer Planets Research (OPR) programs.

## References

- [Albritton, D.L., Dotan, I., Lindinger, W., McFarland, M., Tellinghuisen, J., Fehsenfeld, F. C., 1977.](#) Effects of ion speed distributions in flow drift tube studies of ion-neutral reactions. *Journal of Chemical Physics* 66, 410.
- [Alexander, C., Carlson, R., Consolmagno, G., Greeley, R., Morrison, D., 2009.](#) In: [Pappalardo, R., McKinnon, W.B., Khurana, K. \(Eds.\), The Exploration History of Europa](#), in *Europa*. U. of Arizona Press, pp. 3–26.

- Amsif, A., Dandouras, J., Roelof, E.C., 1997. Modeling the production and the imaging of energetic neutral atoms from Titan's exosphere. *Joe Gibbs Racing* 102 (22), 169.
- Anicich, V.G., 1993. Evaluated bimolecular ion-molecule gas phase kinetics of positive ions for use in modeling planetary atmospheres, cometary comae, and interstellar clouds. *Journal of Physical and Chemical Reference Data* Vol. 22 (No.6).
- Bagenal, F., Sullivan, J.D., 1981. Direct plasma measurements in the Io torus, and inner magnetosphere. *Journal of Geophysical Research* 86, 8447–8466.
- Bale, S.D., Ullrich, R., Goetz, K., Alster, N., Cecconi, B., Dekkali, M., Lingner, N.R., Macher, W., Manning, R.E., McCauley, J., Monson, S.J., Oswald, T.H., Pulupa, M., 2008. The electric antennas for the STEREO/WAVES experiment. *Space Science Reviews* 136, 529–547, <http://dx.doi.org/10.1007/s11214-007-9251>.
- Banks, P.M., Kockarts, G., 1973. *Aeronomy*. Academic, San Diego, Calif.
- Belcher, J.W., 1983. The low-energy plasma in the Jovian magnetosphere. In: Dessler, A.J. (Ed.), *Physics of the Jovian Magnetosphere*, 68. Cambridge University Press.
- Belton, M.J.S., et al., New Frontiers in the Solar System—An Integrated Exploration Strategy, Solar System Exploration Survey, Space Studies Board, National Research Council, July 9, 2002.
- Blackburn, K., B., Lessard, D., Kirchner, W. Kurth, Controlling Low Frequency Interference from Direct Energy Transfer Spacecraft Power Systems, 978-1-4577-0811-4/11/2011 IEEE, 2011, pp. 840–845.
- Bridge, et al., 1979a. Plasma observations near Jupiter: initial results from Voyager 1. *Science* 204, 987–991.
- Bridge, et al., 1979b. Plasma observations near Jupiter: initial results from Voyager 2. *Science* 206, 972–976.
- Broadfoot, et al., 1979. Extreme ultraviolet observations from Voyager 1 encounter with Jupiter. *Science* 204, 979–982.
- Brzezinski, M.A., 1985. The Si:C:N ratio of marine diatoms: interspecific variability and the effect of some environmental variables. *Journal of Phycology* 21, 347–357.
- Carlson, R.W., Johnson, R.E., Anderson, M.S., 1999. Sulfuric acid on Europa and the radiolytic sulfur cycle. *Science* 286, 97–99.
- Carlson, R.W., Anderson, M.S., Johnson, R.E., Schulman, M.B., Yavrouian, A.H., 2002. Sulfuric acid production on Europa: the radiolysis of sulfur in water ice. *Icarus* 157, 456–463.
- Carlson, R.W., Calvin, W.M., Dalton, J.B., Hansen, G.B., Hudson, R.L., Johnson, R.E., McCord, T.B., Moore, M.H., 2009. In: Pappalardo, R., McKinnon, W.B., Khurana, K. (Eds.), *Europa's Surface Composition*, Europa. U. of Arizona Press, pp. 283–327.
- Cassidy, T.A., et al., 2007. The spatial morphology of Europa's near-surface O<sub>2</sub> atmosphere. *Icarus* 191, 755–764.
- Cassidy, T.A., Johnson, R.E., Geissler, P.E., Leblanc, F., 2008. Simulation of Na D emission near Europa during eclipse. *Journal of Geophysical Research* 113, E02005, <http://dx.doi.org/10.1029/2007JE002955>.
- Cassidy, T.A., Johnson, R.E., Tucker, O.J., 2009. Trace constituents of Europa's atmosphere. *Icarus* 201, 182–190.
- Clark, K., et al., Europa Jupiter System Mission Joint Summary Report, Jan. 16, 2009, Joint Jupiter Science Definition Team, NASA/ESA Study Team, 2009.
- Coates, A.J., Wellbrock, A., Lewis, G.R., Cray, F.J., Young, D.T., Thomsen, M.F., Szego, K., Bebes, Z., Arridge, C.S., Jones, G.H., Sittler Jr., E.C., 2012. Cassini in Titan's tail: CAPS observations of plasma escape. *Journal of Geophysical Research* 117, A05324, <http://dx.doi.org/10.1029/2012JA017595>.
- Cooper, J.F., Johnson, R.E., Mauk, B.H., Garrett, H.B., Gehrels, N., 2001. Energetic ion and electron irradiation of the icy Galilean satellites. *Icarus* 149, 133–159.
- Dalton, J.B., Cruikshank, D.P., Stephan, K., McCord, T.B., Coustenis, A., Carlson, R.W., Coradini, A., 2010. Chemical composition of icy satellite surfaces. *Space Science Reviews* 153, 113–154.
- Doggett, T., Greeley, R., Figueredo, P., Tanaka, K., 2009. In: Pappalardo, R., McKinnon, W.B., Khurana, K. (Eds.), *Geologic Stratigraphy and Evolution of Europa's Surface*, Europa. U. of Arizona Press, pp. 137–159.
- Ergun, R.E., Malaspina, D.M., Bale, S.D., McFadden, J.P., Larson, D.E., Mozer, F.S., Meyer-Vernet, N., Maksimovic, M., Kellogg, P.J., Wygant, J.R., 2010. Spacecraft charging and ion wake formation in the near-Sun environment. *Physics of Plasmas* 17 (072903), 1–9.
- Eviatar, A., Vasyliunas, V.M., Gurnett, D.A., 2001. The ionosphere of Ganymede. *Planetary and Space Science* 49, 327–336.
- Frank, L.A., Paterson, W.R., Ackerson, K.L., Bolton, S.J., 1997. Outflow of hydrogen ions from Ganymede. *Geophysical Research Letters* 24, 2151.
- Greeley, R., Chyba, C.F., Head III, J.W., McCord, T.B., McKinnon, W.B., Pappalardo, R.T., Figueredo, P.H., 2004. The geology of Europa, in Jupiter—the planet. In: Bagenal, F., McKinnon, W.B., Dowling, T.E. (Eds.), *Satellites and Magnetosphere*. Cambridge Univ. Press, pp. 329–362.
- Greeley, R., Pappalardo, R.T., Prockter, L.M., Hendrix, A.R., Luck, R.E., 2009. In: Pappalardo, R., McKinnon, W.B., Khurana, K. (Eds.), *Future Exploration of Europa*, in Europa. U. of Arizona Press, pp. 655–695.
- Hall, D.T., Strobel, D.F., Feldman, P.D., McGrath, M.A., Weaver, H.A., 1995. Detection of an oxygen atmosphere on Jupiter's moon Europa. *Nature* 373, 677–679.
- Hall, D.T., Feldman, P.D., McGrath, M.A., Strobel, D.F., 1998. The far ultraviolet oxygen airglow of Europa and Ganymede. *The Astrophysical Journal* 499, 475–481.
- Hammock, C.M., C.P. Paranicas, N.P. Paschalidis. Europa radiation environment and monitoring. In: *Proceedings IEEE Aerospace Conference*, ISBN 978-1-4244-2621-8, 24 April 2009a.
- Hand, K.P., Chyba, C.F., Priscu, J.C., Carlson, R.W., Nealson, K.H., 2009. In: Pappalardo, R., McKinnon, W.B., Khurana, K. (Eds.), *Astrobiology and the Potential for Life on Europa*, in Europa. U. of Arizona Press, pp. 589–629.
- Hand, K.P., Chyba, C.F., Carlson, R.W., Cooper, J.F., 2006. Clathrate Hydrates of Oxidants in the Ice Shell of Europa. *Astrobiology* 6 (3), 463–482.
- Hartle, R.E., Killen, R., 2006. Measuring pickup ions to characterize the surfaces and exospheres of planetary bodies: applications to the Moon. *Geophysical Research Letters* 33, L05201, <http://dx.doi.org/10.1029/2005GL024520>.
- Hartle, R.E., Sittler Jr., E.C., 2007. Pickup ion phase space distributions: effects of atmospheric spatial gradients. *Journal of Geophysical Research* 112, A07104.
- Hartle, R.E., Sarantos, M., Sittler Jr., E.C., 2011. Pickup ion distributions from three-dimensional neutral exospheres. *Journal of Geophysical Research* 116, A10101, <http://dx.doi.org/10.1029/2011JA016859>.
- Hammock, C.M., C.P. Paranicas, N.P. Paschalidis. Europa radiation environment and monitoring. In: *Proceedings IEEE Aerospace Conference*, ISBN 978-1-4244-2621-8, April 24, 2009b.
- Huebner, W.F., Giguere, P.T., 1980. A model of comet comae, II, Effects of solar photodissociation ionization. *Astrophysics Journal* 238, 753.
- Ip, W.H., Williams, D.J., McEntire, R.W., Mauk, B.H., 1998. Ion sputtering and surface erosion at Europa. *Geophysical Research Letters* 25, 829–832.
- Johnson, R.E., Burger, M.H., Cassidy, T.A., Leblanc, F., Marconi, M., Smyth, W.H., 2009. In: Pappalardo, R., McKinnon, W.B., Khurana, K. (Eds.), *Composition and Detection of Europa's Sputter-induced Atmosphere*, Europa. U. of Arizona Press, pp. 507–527.
- Johnson, R.E., Lanzerotti, L.J., Brown, W.L., 1982. Planetary applications of ion induced erosion of condensed-gas frosts. *Nuclear Instruments and Methods* 198, 147–157.
- Johnson, R.E., 1990. *Energetic Charged-Particle Interactions with Atmospheres and Surfaces*. Springer-Verlag, Berlin.
- Johnson, R.E., Carlson, R.W., Cooper, J.F., Paranicas, C., Moore, M.H., Wong, M.C., 2004. Radiation effects on the surfaces of the Galilean satellites. In: Bagenal, F., Dowling, T., McKinnon, W. (Eds.), *Jupiter: Satellites, Atmosphere, Magnetosphere*. Cambridge Univ. Press, New York, pp. 483–510.
- Kabin, K., Combi, M.R., Gombosi, T.I., Nagy, A.F., DeZeeuw, D.L., Powell, K.G., 1999. *Journal of Geophysical Research* 104 (A9), 19983–19992.
- Khurana, K.K., Kivelson, M.G., Stevenson, D.J., Schubert, G., Russell, C.T., Walker, R.J., Polanskey, C., 1998. Induced magnetic fields as evidence for subsurface oceans in Europa and Callisto. *Nature* 395, 777–780.
- Kivelson, M.G., Khurana, K.K., Stevenson, D.J., Bennett, L., Joy, S., Russell, C.T., Walker, R.J., Zimmer, C., Polanskey, C., 1999. Europa and Callisto: induced or intrinsic fields in a periodically varying plasma environment. *Journal of Geophysical Research* 104 (A3), 4609–4625.
- Kivelson, M.G., Khurana, K.K., Russell, C.T., Volwerk, M., Walker, R.J., Zimmer, C., 2000. Galileo magnetometer measurements: a stronger case for a subsurface ocean at Europa. *Science* 289, 1340–1343.
- Khurana, K.K., Kivelson, M.G., Hand, K.P., Russell, C.T., 2009. In: Pappalardo, R., McKinnon, W.B., Khurana, K. (Eds.), *Electromagnetic Induction from Europa's Ocean and Deep Interior*, Europa. U. of Arizona Press, pp. 571–586.
- Kivelson, M.G., et al., 2006. In: Bagenal, F., Dowling, T., McKinnon, W. (Eds.), *Magnetospheric Interactions with Satellites, Jupiter, The Planet, Satellites and Magnetosphere*. Cambridge Planetary Science, pp. 513–536, Chapter 21.
- Kivelson, M.G., Khurana, K.K., Volwerk, M., 2009. In: Pappalardo, R., McKinnon, W.B., Khurana, K. (Eds.), *Europa's Interaction with the Jovian Magnetosphere*, Europa. U. of Arizona Press, pp. 545–570.
- Kliore, A., et al., 1997. The ionosphere of Europa from Galileo radio occultations. *Science* 277, 355.
- Koldoba, A.V., Romanova, M.M., Ustyugova, G.V., Lovelace, R.V.E., 2002. Three dimensional MHD simulation of accretion to an inclined rotator: the “cubed sphere” method. *Astrophysics Journal* 576, L53–L56.
- Krimigis, S.M., Carbary, J.F., Keath, E.P., Bostrom, C.O., Axford, W.I., Gloeckler, G., Lanzerotti, L.J., Armstrong, T.P., 1981. Characteristics of the hot plasmas in the Jovian magnetosphere: results from the Voyager spacecraft. *Journal of Geophysical Research* 86, 8227.
- Lipatov, A.S., Cooper, J.F., Paterson, W.R., Sittler, E.C., Hartle, R.E., 2010. Jovian's plasma torus interaction with Europa: 3D hybrid kinetic simulation. *First Results, Planetary and Space Science* 58, 1681–1691.
- Lipatov, A.S., Cooper, J.F., Paterson, W.R., Sittler, E.C. Jr., Hartle, R.E., Simpson, D.G., 2013. Jovian plasma torus interaction with Europa. Plasma wave structure and effect of inductive magnetic field: 3D Hybrid kinetic simulation. *Planetary and Space Science* 77, 12–24.
- Lipatov, A.S., Sittler, E.C. Jr., Hartle, R.E., Cooper, J.F., 2012. Short wave length electromagnetic perturbations excited near the solar probe plus spacecraft in the inner heliosphere: 2.5D hybrid modeling. *Planetary and Space Science* 62, 61–68.
- Mauk, B.H., Gary, S.A., Kane, M., Keath, E.P., Krimigis, S.M., Armstrong, T.P., 1996. Hot plasma parameters of Jupiter's inner magnetosphere. *Journal of Geophysical Research* 101, 7685–7695.
- Mauk, B.H., Mitchell, D.G., McEntire, R.W., Paranicas, C.P., Roelof, E.C., Williams, D.J., Krimigis, S.M., Lagg, A., 2004. Energetic ion characteristics and neutral gas interactions in Jupiter's magnetosphere. *Journal of Geophysical Research* 109, A09S12, <http://dx.doi.org/10.1029/2003JA010270>.
- Maynard, N.C., 1998. Electric field measurements in moderate to high density space plasmas with passive double probes. In: Pfaff, R.F., Borovsky, J.E., Young, D.T. (Eds.), *AGU Geophysical Monograph*, vol. 103; 1998, pp. 13–27.
- McCord, T.B., et al., 1998. Salts on Europa's surface detected by Galileo's Near Infrared Mapping Spectrometer. *Science* 280, 1242–1245.

- McCord, T.B., et al., 1999. Hydrated salt minerals on Europa's surface from the Galileo near-infrared mapping spectrometer (NIMS) investigation. *Journal of Geophysical Research* 104, 11827–11851.
- McGrath, M.A., Hansen, C.J., Hendrix, A.R., 2009. In: Pappalardo, R., McKinnon, W.B., Khurana, K. (Eds.), *Observations of Europa's Tenuous Atmosphere*. Europa. U. of Arizona Press.
- McGrath, M.A., Lellouch, E., Strobel, D.F., Feldman, P.D., Johnson, R.E., 2004. Satellite atmospheres. In: F. Bagenal, W. McKinnon, T. Dowling, (Eds.), *Jupiter: Satellites, Atmosphere, Magnetosphere*. Cambridge Univ. Press, Cambridge, pp. 457–483.
- McEwen, A.S., Keszthelyi, L.P., Lopes, R., Schenk, P.M., Spencer, J.R., 2006. In: Bagenal, F., Dowling, T., McKinnon, W. (Eds.), *The Lithosphere and Surface of Io, Jupiter The Planet, Satellites and Magnetosphere*. Cambridge Planetary Science, pp. 307–328, Chapter 14.
- McNutt, R.L., Belcher, J.W., Bridge, H.S., 1981. Positive ion observations in the middle magnetosphere of Jupiter. *Journal of Geophysical Research* 86, 8319–8342.
- Plainaki, C., Milillo, A., Mura, A., Orsini, S., Massetti, S., Cassidy, T., 2012. The role of sputtering and radiolysis in the generation of Europa exosphere. *Icarus* 218, 956–966.
- Pappalardo, R.T., Belton, M.J.S., Breneman, H.H., Carr, M.H., Chapman, C.R., Collins, G.C., Denk, T., Fagents, S., Geissler, P.E., Giese, B., Greeley, R., Greenberg, R., Head, J.W., Helfenstein, P., Hoppa, G., et al., 1999. Does Europa have a subsurface ocean? Evaluation of the geological evidence. *Journal of Geophysical Research* 104, 24015–24055.
- Paranicus, C., Cooper, J.F., Garrett, H.B., Johnson, R.E., Sturmer, S.J., 2009. In: Pappalardo, R., McKinnon, W.B., Khurana, K. (Eds.), *Europa's Radiation Environment and Its Effects on the Surface*, in Europa. U. of Arizona Press, pp. 529–544.
- Pasek, M.A., Greenberg, R., 2012. Acidification of Europa's subsurface ocean as a consequence of oxidant delivery. *Astrobiology* 12, 151–159.
- Paterson, W.R., Frank, L.A., Ackerson, K.L., 1999. Galileo plasma observations at Europa and Moments. *Journal of Geophysical Research* 104 (A10), 22,779–22,791.
- Pedersen, A., F. Mozer, G. Gustafsson, *Electric Field Measurements in a Tenuous Plasma with Spherical Double Probes*. AGU Geophysical Monograph, (Eds.) R. F. Pfaff, J. E. Borovsky, D. T. Young, vol. 103, pp. 1–12, 1998.
- Sandel, et al., 1979. Extreme ultraviolet observations from Voyager 2 encounter with Jupiter. *Science* 206, 962–966.
- Saur, J., Strobel, D.F., Neubauer, F.M., 1998. Interaction of the jovian magnetosphere with Europa: constraints on the atmosphere. *Journal of Geophysical Research* 103, 19947–19962.
- Schaefer, L., Fegley Jr., B., 2005a. Alkali and halogen chemistry in volcanic gases on Io. *Icarus* 173, 454–468.
- Schaefer, L., Fegley Jr., B., 2005b. Predicted abundances of carbon compounds in volcanic gases on Io. *Astrophysics Journal* 618, 1079–1085.
- Schilling, N., Neubauer, F.M., Saur, J., 2007. Time-varying interaction of Europa with the Jovian magnetosphere: constraints on the conductivity of Europa's subsurface ocean. *Icarus* 192, 41–55.
- Schilling, N., Neubauer, F.M., Saur, J., 2008. Influence of the internally induced magnetic field on the plasma interaction of Europa. *Journal of Geophysical Research (Space Physics)* 113, 3203.
- Shematovich, V.I., Johnson, R.E., Cooper, J.F., Wong, M.C., 2005. Surface bounded atmosphere of Europa. *Icarus* 173, 480–498.
- Sittler, E.C., Strobel, D.F., 1987. Io plasma torus electrons: Voyager 1. *Journal of Geophysical Research* 92 (A6), 5741–5762.
- Sittler Jr., E.C., Johnson, R.E., Jurac, S., Richardson, J.D., McGrath, M., Cray, F., Young, D.T., Nordholt, J.E., 2004. Pickup ions at Dione and Enceladus: Cassini plasma spectrometer simulations. *Journal of Geophysical Research* 109, A01214, <http://dx.doi.org/10.1029/2002JA009647>.
- Sittler Jr., E.C., Hartle, R.E., Viñas, A.F., Johnson, R.E., Smith, H.T., 2005. Titan interaction with Saturn's magnetosphere: Voyager 1 results revisited. *Journal of Geophysical Research* 110, A09302, <http://dx.doi.org/10.1029/2004JA010759>.
- Sittler Jr., E.C., Thomsen, M., Johnson, R.E., Hartle, R.E., Burger, M., Chornay, D., Shappirio, M.D., Simpson, D., Smith, H.T., Coates, A.J., rymer, A.M., McComas, D. J., Young, D.T., Reisenfeld, D., Dougherty, M., Andre, N., 2006. Cassini observations of Saturn's inner plasmasphere: Saturn orbit insertion results. *Planetary and Space Science* 54, 1197–1210.
- Sittler Jr., E.C., Hartle, R.E., Johnson, R.E., Cooper, J.F., Lipatov, A.S., Bertucci, C., Coates, A.J., Szego, K., Shappirio, M., Simpson, D.G., Wahlund, J.-E., 2010. Saturn's magnetospheric interaction with Titan as defined by Cassini encounters T9 and T18: new results. *Product service system*, 327–350.
- Smith, B.A., et al., 1979. The Jupiter system through the eyes of Voyager 1. *Science* 204, 951–957.
- Smyth, W.H., Marconi, M.L., 2006. Europa's atmosphere, gas tori, and magnetospheric implications. *Icarus* 181, 510–526.
- Spencer, J.R., Tamppari, L.K., Martin, T.Z., Travis, L.D., 1999. Temperatures on Europa from Galileo PPR: nighttime thermal anomalies. *Science* 284, 1514–1516.
- Squyres, S.W., et al., 2011. National Research Council, *Vision and Voyages for Planetary Science in the Decade 2013–2022*. The National Academies Press, Washington, DC.
- Vasyliunas, V.M., Eviatar, A., 2000. Outflow of ions from Ganymede: a reinterpretation. *Geophysical Research Letters* 27, 1347.
- Waite, J.H., Lewis, W.S., Kasprzak, W.T., Anicich, V.G., Block, B.P., Cravens, T.E., Fletcher, G.G., Ip, W.-H., Luhmann, J.G., McNutt, R.L., Niemann, H.B., Parejko, J.K., Richards, J.E., Thorpe, R.L., Walter, E.M., Yelle, R.V., 2004. The Cassini ion and neutral mass spectrometer (INMS) investigation. *Space Science Reviews* 114, 113–231.
- Waite, J.H., Combi, M.R., Ip, W.-H., Cravens, T.E., McNutt, R.L., Kasprzak, W., Yelle, R., Luhmann, J., Niemann, H., Gell, D., Magee, B., Fletcher, G., Lunine, J., Tseng, W.-L., 2006. Cassini ion and neutral mass spectrometer: Enceladus plume composition and structure. *Science* 311, 1419–1422.
- Waite Jr., J.H., Lewis, W.S., Magee, B.A., Lunine, J.I., McKinnon, W.B., Glein, C.R., Mousis, O., Young, D.T., Brockwell, T., Westlake, J., Nguyen, M.-J., Teolis, B.D., Niemann, H. B., McNutt Jr., R., Perry, L.M., Ip, W.-H., 2009. Liquid water on Enceladus from observations of ammonia and <sup>40</sup>Ar in the plume. *Nature* 460, 487–490.
- Williams, D.J., Mauk, B., McEntire, R.W., 1998. Properties of Ganymede's magnetosphere as revealed by energetic particle observations. *Journal of Geophysical Research* 103, 17523–17534.
- Zolotov, M.Y., Shock, E.L., 2001. Composition and stability of salts on the surface of Europa and their oceanic origin. *Journal of Geophysical Research* 106, 32815–32828.
- Zolotov, M.Y., Shock, E.L., 2004. A model for low-temperature biogeochemistry of sulfur, carbon, and iron on Europa. *Journal of Geophysical Research* 109, E06003, <http://dx.doi.org/10.1029/2003JE002194>.